Ph. D. DISSERTATION

STUDY ON THREE-DIMENSIONAL ANAMORPHIC VOLUMETRIC DISPLAY SYSTEM

3차원 왜상 체적형 디스플레이 시스템에 관한 연구

By

GILBAE PARK

AUGUST 2012

SCHOOL OF ELECTRICAL ENGINEERING

AND COMPUTER SCIENCE

COLLEGE OF ENGINEERING

SEOUL NATIONAL UNIVERSITY

Abstract

Study on three-dimensional anamorphic volumetric display system

GILBAE PARK
DEPARTMENT OF ELECTRICAL ENGINEERING AND COMPUTER SCIENCE
COLLEGE OF ENGINEERING
SEOUL NATIONAL UNIVERSITY

This dissertation proposed novel three-dimensional (3D) display systems which use the principle of anamorphosis. There have been many attempts to display three-dimensional information based on various kinds of technologies such as stereoscopic and auto-stereoscopic technologies, volumetric display technology, holography, and so on. The technologies use much bigger amount of information for 3D display than that for 2D display. However, since conventional display devices have limitations in the amount of information to display, many researches for 3D display have used sequential or spatial multiplexing methods.

The author proposes an anamorphic floating display system using a cylindrical mirror and tracking technology. The cylindrical mirror can be used like a convex lens in the polar axis. It means that the cylindrical mirror can float an image from a 2D display panel and a viewer can see the floated image over the cylindrical mirror. To give the parallax in the longitudinal axis to the viewers, the tracking technology will be used to generate the images according to the position of the viewers.

In addition, the author designs an anamorphic volumetric display system using a digital mirco-mirror device (DMD) projector which can project images in high speed, a cylindrical mirror, wedge prisms, and an anisotropic diffuser. The projector can be used to project a large number of directional images to many directions in high speed. And the cylindrical mirror can float images from the projector at the position by the lens formula in the polar axis of the cylindrical mirror. To project directional images to the respective directions, wedge prisms and motor driving are used. A wedge prism can deviate a beam to a different angle in the longitudinal plane from the incident angle. The author drives an electric motor to rotate wedge prisms. The rotation of the wedge prisms makes the deviation angle of the incident images from the wedge prisms change. Deviated images are reflected and distorted by the cylindrical mirror. The image distortion is similar to that in anamorphosis. To correct the distortion caused by the cylindrical mirror, inversely distorted images are generated by processes in five steps and those images are projected to the cylindrical mirror. The exit aperture size and diverging angle of the projector are not big enough to cover the vertical positions of viewers. In other words, a viewer can see only some lines from the projector. To solve this problem, an anisotropic diffuser is attached to the cylindrical mirror, and used to diffuse images in only vertical direction. Specific information and further explanations of each component will be provided and experimental results will be presented for verification.

Keywords: Three-dimensional display, volumetric display, cylindrical mirror, wedge prism, digital micro mirror projector

Student number : 2008- 30874

Contents

List of Figures

List of Tables

1. Introduction

1.1. Contemporary issues on three-dimensional display

Recently, whenever we watch science-fiction films, we cannot only enjoy the films with three-dimensional (3D) images, but we can also watch various kinds of 3D display systems which show 3D images in the films even though the systems are not real yet. 3D display technologies have attracted so much attention from researchers, companies and the public. However, the history of 3D display technologies is not short. Their developmental history dates back to the Wheatstone stereoscope developed by Wheatstone in 1838. The device was the first stereoscope using two images to give binocular disparity. The principle of binocular disparity is not different from that in contemporary commercialized stereoscopic 3D televisions manufactured by consumer electronics companies.

To understand how human percept the depth information in 3D images, we need to know physiological and psychological depth cues of the human visual system (HVS). HVS consists of separate subsystems which operate together after watching a scene. It is known that all visual information from eye is transmitted to the brain through neural paths at the first step of image recognition process. After that, perception of depth information is conducted by separate families of depth cues with varying importance in multiple layers which provide information concerning the depth information of a scene from the eye [1].

In more details about depth cues, physiological depth cues include accommodation with convergence, binocular disparity, and motion parallax. And there are psychological cues like linear perspective, overlapping, shading or shadow, texture gradient, and so on. Among them, since physiological depth cues are independent on the contents on images, the three physiological depth cues are used to show differences in contemporary 3D

display technologies. As Figure 1.1 shows the depth range using different depth cues, the importance of each depth cue varies with the distance from the observer.

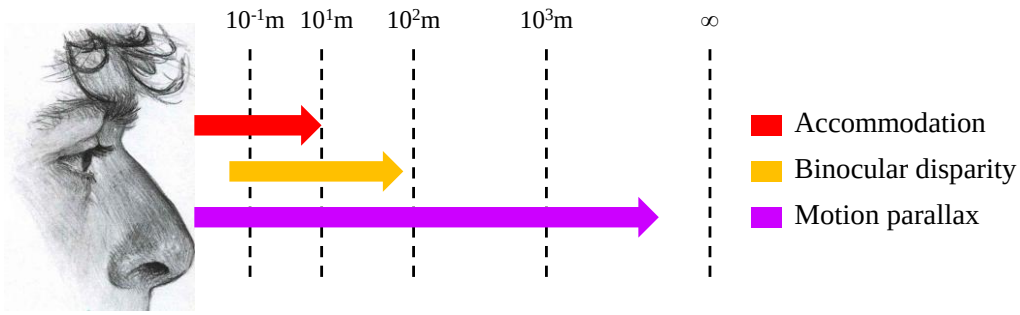

Figure 1.1 The range of depth perception using three physiological depth cues.

Binocular disparity is the most representative depth cues and the easiest way to give observers with two slightly different images. The mechanism of binocular depth estimation has two parts which are vergence and stereopsis [1]. Vergence is the process in which both eyes take positions to minimize the difference of the visual information from two eyes. After the vergence, stereopsis process uses the disparity of two images from two eyes to estimate depth information. Binocular disparity has less importance at too near distance for two eyes to focus simultaneously.

At the very short distance, accommodation is the primary depth cue because the change in refraction power of eyes can be relatively bigger than in not short distance. The problem results from the discordance with information in other depth cues. The phenomenon is so called accommodation-convergence rivalry.

Lastly, motion parallax is a depth cues to estimate depth information using the change in parallaxes of a moving object. There should be relative motions to get depth information with motion parallax. However, only motion parallax among physiological cues affects human in almost distant range, and is the last clue to give certainty of depth data.

Basically, a stereoscopic 3D display technology provides two images to two eyes simultaneously with two different types of polarized eyeglasses, or alternatively with

shutter glasses. Up to now, these technologies are the best to provide 3D images with high resolution, large viewing region, and economic feasibility. However, stereoscopic 3D display systems can use only binocular disparity to transport depth information to observers. Hence the estimated depth information from binocular disparity collides with the other depth information from other cues like accommodation and motion parallax, which is the major cause of discomforts of 3D images in stereoscopic 3D display systems.

Besides stereoscopic 3D display technologies, various technologies for 3D displaying have been developed and refined for more than one hundred years. Those are multi-view displays, integral imaging, super multi-view displays, volumetric displays and holographic displays. Figure 1.2 shows the types 3D displays and which depth cues can be used in the 3D displays.

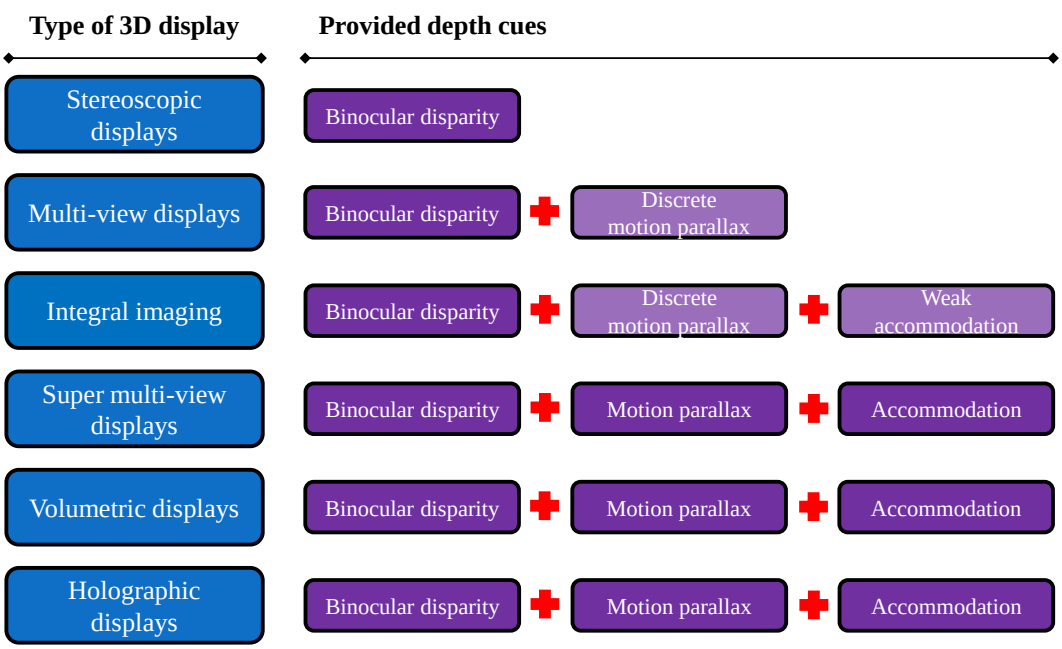

Figure 1.2 3D displays and the depth cues they provide.

Multi-view displays provide a discrete set of perspective view images using a parallax barrier or a lenticular sheet. According to the super multi-view condition [2, 3], if the

sampling interval of parallax on reproduced images is narrower than pupil size, there can be no conflict between accommodation and vergence information. However, super multi-view systems using large number of projectors are very bulky and expensive to implement.

Holography also provides all depth cues and is often called the ultimate 3D technique. Holographic displays reconstruct the light field of real scenes by diffraction of coherent light with a spatial light modulator with very fine pixel pitch about several micrometers. But the disadvantages of holography displays is in technical difficulties including that it is hard to make spatial light modulators with one or sub-micron pixel pitch to expand viewing angle.

Volumetric displays do not use a single screen, but use an enclosed 3D volume to show 3D images with a wide viewing range like 360 degrees, and three depth cues including accommodation cue. Volumetric displays use commonly high-speed projectors or large number of projectors to project more than one hundred view images. In the case of volumetric images, they provide continuous parallax in just front of any number of observers from any distance besides correct accommodation cue. They are more natural images because of no accommodation-convergence rivalry.

1.2. Comparison of volumetric display systems

There have been various approaches in the implementation of volumetric display systems about for a century [2]. Volumetric display can provide almost all 3D depth cues that were mentioned above. It results from the characteristics of volumetric displays such as 3D images from emission, scattering, or relaying of illumination from a set of localized regions [5]. The small localized region or volume in space is called a voxel or a volumetric pixel which means the minimum volume element to display a point in 3D space corresponding to a pixel in two-dimensional image.

Although there is no standardization for implementation of volumetric display systems, those can be classified with types of image volume. Two types of the volume are static-

volume type and swept-volume type. Static volume type volumetric 3D displays create 3D images without any moving parts. For the materials which are used in the static volume type volumetric displays, a stack of liquid crystal scattering shutters [4], a crystal or glass [7-9], gas like fog [5] have been used. It is more difficult to extend the image volume because of limitation of each material.

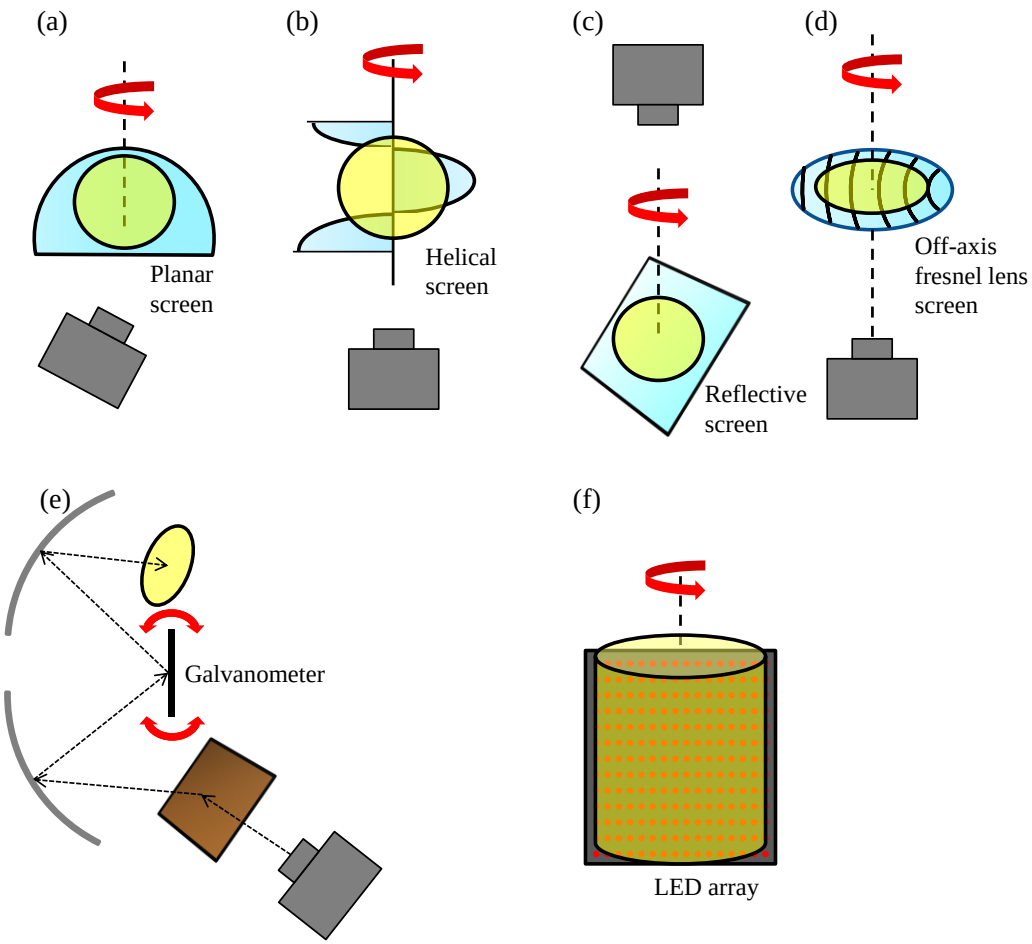

Figure 1.3 Various types of volumetric display system using one or two projectors, or light emitting diodes. Yellow areas mean the rough sizes and positions of the image volume in the systems.

Meanwhile, swept volume type volumetric display has advantages in that it is easier to

modify the shape of rotating screens or mirrors with various optical elements. Figure 1.3 shows contemporary various types of swept volume type volumetric displays. The yellow regions mean the position and the size of each image volume roughly. As shown in Figure 1.3(a)-(d), the rotation of two-dimensional screens is commonly used to make swept volume with rotating planes [11-14]. The sizes of swept volume are defined with the size of rotating screens. However, the rotation speed should be higher than 1200 rpm because these systems use the principle of persistence of vision. The existence of moving parts in such high speed makes strong vibrations, heavy equipment for less vibration and safety. Moreover, this fact can be a limitation for larger image volume.

Figure 1.3(e) shows the brief structure using a comparatively small galvanometer for scanning multiple planes over a space with two concave mirrors [15]. This system has advantages in minimizing moving parts to reduce the danger with vibration. However, the fast repetitive motion of the galvanometer can make it difficult to float large image planes without aberrations from mirrors or lenses.

The last one, Figure 1.3(f) shows the 3D system using rotating two-dimensional light emitting diode (LED) arrays [16]. The characteristics of this system are that it needs no projector but LED arrays, and the resolution of the image volume is defined by the number of LEDs. The number of LEDs cannot be very large because there is a limitation in the amount of the electric current to LEDs and the LED array panel should also rotate in high speed with safety.

1.3. Overview of anamorphosis

Perspective view or perspective projection is made from the viewing volume from the pupil of eyes or cameras. The human always see the world using perspective without any intention. The novel representation of perspective using the simple principle of reflection on the plane, cone, and cylinder is called anamorphosis. Anamorphosis or anamorphic projection is a kind of distortion for distorted images which appear normal only when

observed from a particular position [17]. Anamorphosis has been used to produce artistic images in illusory ways since sixteenth century [18, 19].

The numerical transformations of two dimensional images by an oblique plane, a cone-shaped mirror, and an outer surface of cylindrical mirror are described in [17]. Figure 1.4 shows a sign on the road which uses a planar anamorphic transformation to be seen as an orthogonal sign to drivers. Similar transformations on the oblique plane against the optics axis are used to generate images which make illusion images to observers [9]. And Figure 1.5 shows the geometric matrix for cylindrical anamorphosis in seventeenth century and a contemporary example used in an application for kid with a cartoon. Such anamorphic images can also be made with custom images by a free software [21].

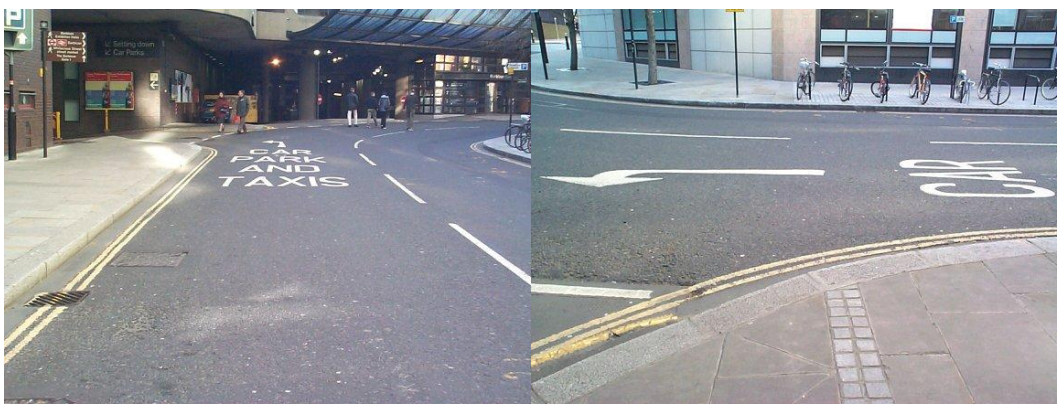

Figure 1.4 A simple example of anamorphosis on the road.

(a) (b)

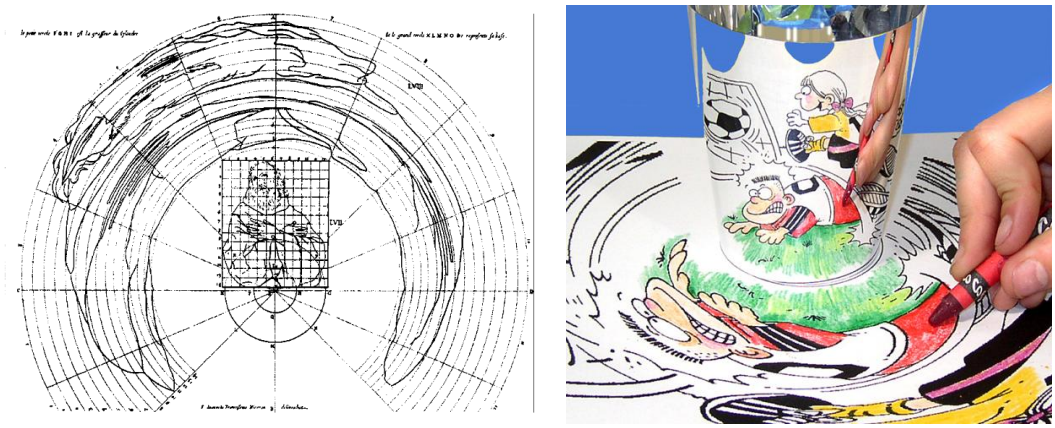

Figure 1.5 (a) Geometric matrix for cylindrical anamorphs by J.-F. Niceron (1638) [17], (b) an example of the cylindrical anamorphs in a cartoon [22].

1.4. Motivation of this dissertation

Despite being used widely with much economical prices, stereoscopic 3D display technologies have not been accepted as the ultimate step of 3D displays, but an intermediate step to other types of 3D displays without no aiding glasses. It is because stereoscopic 3D display technologies can satisfy only binocular disparity among main three depth cues, and accommodation-convergence rivalry phenomenon when watching 3D images for long time ingenerates serious eye fatigue to the observers. The key point for next generation of 3D display seems to be on how 3D display technology can satisfy all kinds of depth cues.

Flat panel display (FPD) devices including liquid crystal display (LCD), plasma display panel (PDP), and organic light emitting diode (OLED) have been used to make 3D display devices with parallax barriers, lenticular sheets, lens arrays, and other many kinds of optic elements. The most of 3D display techniques using FPD devices are focused on multi-view displays which provide a discrete set of directional images. It is certain that FPD devices have been enhanced to scatter light with wide angle both horizontally and vertically. However, 3D images should have directional property. The

scattered light from the FPD devices should lose the scattering property again by parallax barriers, lenticular sheets, pin-hole arrays, lens-arrays, etc.

It is said that there should be more two view images in an eye pupil whose diameter is 2~6 mm to satisfy one of depth cues, accommodation [2, 3], and to provide smooth motion parallax [23]. However, in the case of FPD devices, the limitation of resolution matters more than projection devices since it is more difficult to increase the frame rate. The relatively lower frame rates of FPD devices are resulted from the capacity of electrode on the panels.

On the other hand, projection devices including LCD projector, liquid crystal on silicon (LCoS) projector, and digital micro-mirror device (DMD) projector have advantages on higher frame rates. Among them, some DMD projectors can project images at the frame rate higher than 10,000 fps when using binary images. Therefore, DMD projectors have been widely used to implement various types of volumetric displays because the high frame rate let the system have less falling-off of the image resolution by time-sequential multiplexing method.

Demonstrated volumetric display systems have used rotating screens or mirrors as shown in Figure 1.3(a)-(d) and (f). The rotating speed of them is more than 20 revolutions per second, which can be dangerous to observers. Therefore, the system should have heavy components for the safety with a specific rotating part. Moreover, it is not possible to handle or point on the image volume.

In short, the goal of this dissertation is to design and implement volumetric display systems which have five characteristics as follows.

- 3D images which can be seen in every horizontal direction
- Compact system with a DMD projector
- Minimization of moving parts for safety
- Tangible image volume
- Displaying real objects

1.5. Scope and organization

This dissertation focused on the studies for the practical implementation of anamorphic volumetric display systems using cylindrical mirrors. There are two anamorphic display systems using cylindrical mirrors. One is anamorphic floating display system using a monitor and tracking techniques, the other one is anamorphic volumetric display system using a high-speed DMD projector and rotating wedge prisms.

This dissertation is organized as follows. In Chapter 2, the process for implementing anamorphic floating display system is included. The process consists of anamorphic transformation in the reflection on a cylindrical mirror from two-dimensional images on a monitor, tracking technology with an infrared camera and infrared markers to track the positions of an observer.

Chapters 3 and 4 cover base image generation and the implementation of anamorphic volumetric display system using a DMD projector and rotating wedge prisms respectively. In Chapter 3, five steps for base image generation for the input images in the volumetric display system are explained in detail. Chapter 4 includes detail explanations of each component in the system including a DMD projector, wedge prisms with a motor driving part, a cylindrical mirror with an anisotropic diffuser, etc.

In Chapter 5, the analysis of design parameters and the size of image volume is conducted. And the relationship between the number of view images and super multi-view condition is shown with the expectation of applications.

Finally, a conclusion is provide in Chapter 6.

2. Anamorphic floating display with tracking technology

2.1. Anamorphic transformation on two-dimensional images by a cylindrical mirror

Cylindrical anamorphosis is a simple example for display, using a cylindrical mirror or other surfaces. However it shows just a two-dimensional (2D) static image using distorted projection to generate a normal image to the outside of a cylindrical mirror. On the other hand, a toy named 'Mirage' provides very clear 3D images with two concave parabolic mirrors [13]. But the 3D image in Mirage comes from a real 3D object with a parabolic mirror.

In this chapter, tracking technology is used to provide floating 2D images having motion parallax with the observer's tracked position. The tracking technology can find the position of an observer almost in real time, and the position information can be used to generate the right view image for the direction from the observer to the 3D objects.

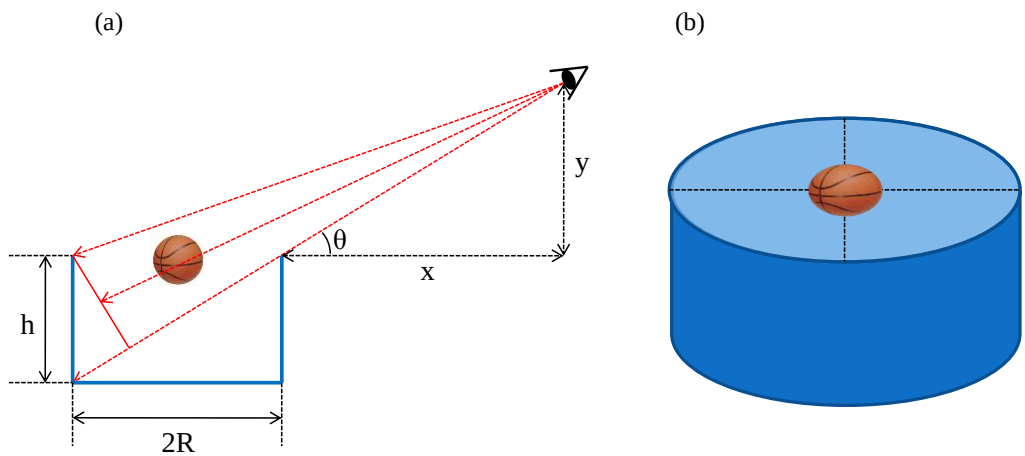

Figure 2.1 The schematic of anamorphic floating display system. (a) Main parameters concerned with the floating image, (b) a floating image on the cylindrical mirror

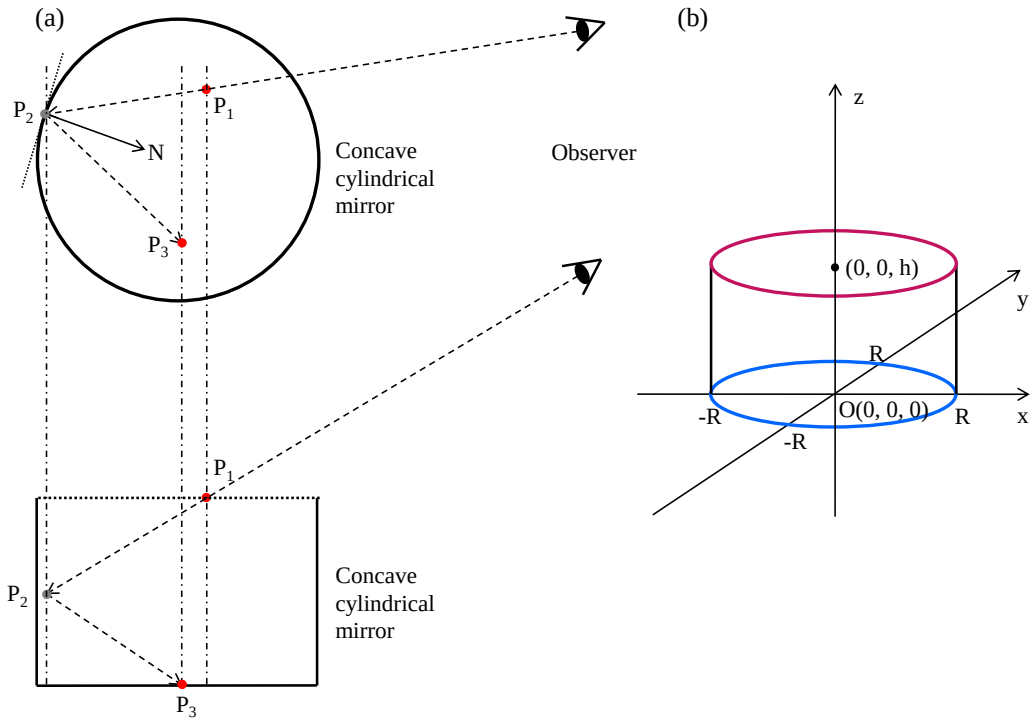

Figure 2.2 (a) Cartesian coordinates system used in image mapping for concave cylindrical mirror, (b) some main points and rays for ray tracing in *xy*-plane and *xz*-plane.

3D Cartesian coordinates can be assumed as shown in Figure 2.2(a) for convenience of calculating mapping points. It means that the polar axis of the cylindrical mirror is *z*-axis and the longitudinal plane is *xy*-plane. The cylindrical mirror behaves like a concave mirror or a convex lens in *xy*-plane, a plane mirror in *z*-axis. Therefore, when an observer watches the inner side of the cylindrical mirror, an arbitrary ray from the observer goes through 3 points like Figure 2.2(b). The points are P_1 on the upper plane, P_2 on the inner side, and P_3 on the bottom plane of the cylindrical mirror. The ray reflects regularly on the inner side of the cylindrical mirror. The reflected direction P_2P_3 can be calculated with Eq. (1). N is the unit normal vector on the point P_2.

$$\overrightarrow{P_2P_3} = 2((N \cdot \overrightarrow{P_1P_2})N) - \overrightarrow{P_1P_2} \quad (1)$$

Provided that an observer stands on (0, -500, 500) mm in the Cartesian coordinates system, we can calculate mapped points of all white points of an original grid image like

Figure 2.3(a). Figure 2.3(b) is the mapped result from the original grid, which shows the different interval depending on the points and flipping of a white square. This result can be applied to a virtual object image made by computer graphics as shown in Figure 2.3(c) and (d).

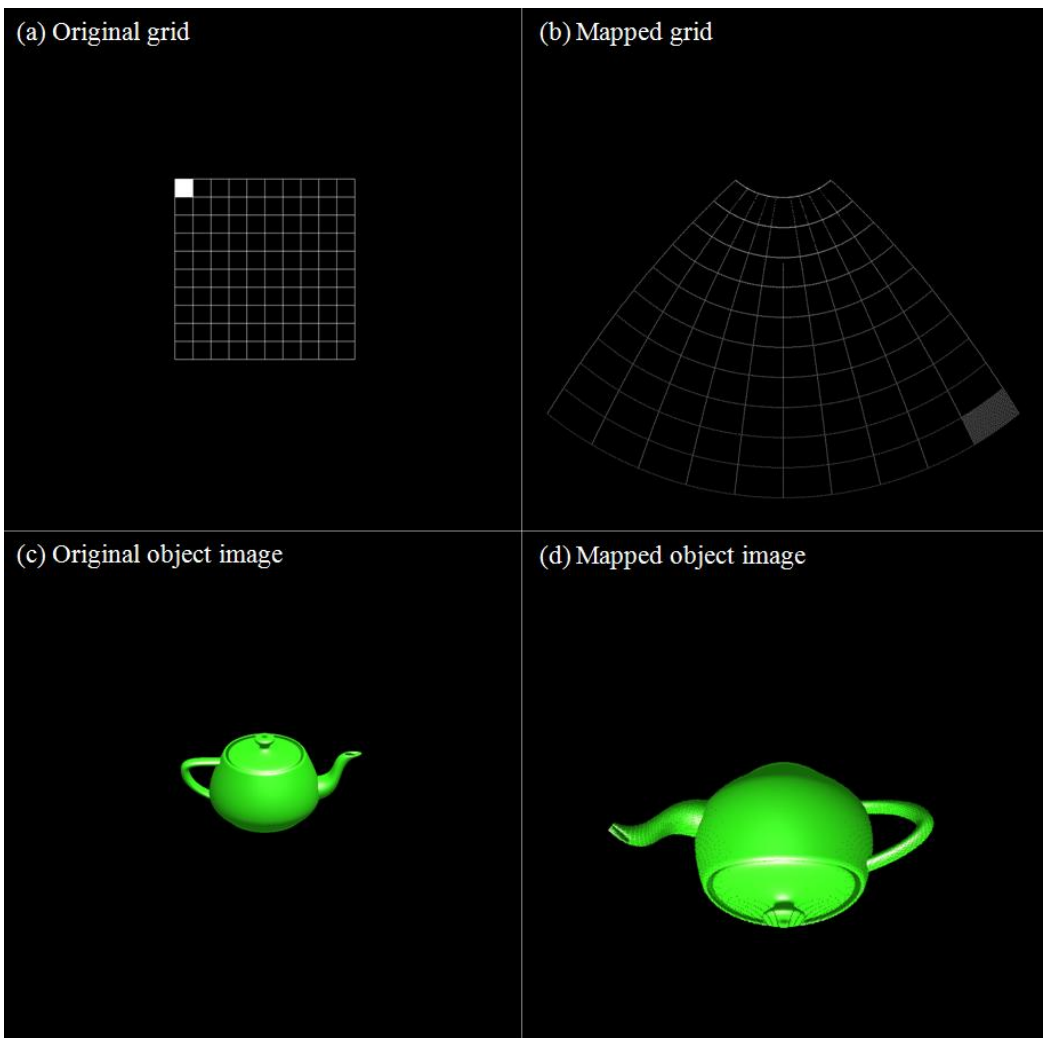

Figure 2.3 (a) Original grid, (b) mapped grid, (c) original object image, and (d) mapped object image, when an observer is at (0, -500, 500) mm from the center point of a cylindrical mirror.

2.2. Omni-directional tracking technology by a convex mirror

In the traditional various systems, tracking technologies are used to make interactions with users by recognizing the position or the velocity of the users. Especially, numerous virtual reality systems such as the CAVE™ and Workbench apply tracking technology to implement the motion parallax which is an important element for spatial cognition [25, 26]. Furthermore, tracking is used to enhance the weak points of hologram like small display size, narrow viewing angle, etc [27].

Although there are many ways for tracking like face recognition, marker recognition, and so on, infrared light emitting diodes (LEDs) are used as markers for the position of an observer in our system. The infrared LED for markers has advantages in that it is very easy to recognize without significant image processes. Figure 2.4(a) shows a goggle equipped with two infrared LEDs with a battery and a power switch. The infrared LEDs emit infrared light whose wavelength is 940 nm. And the infrared camera is modified from a generic web camera, Logitech™ Quickcam-IM with an infrared filter. The infrared camera is shown in Figure 2.4(b). An image from the infrared camera is shown in Figure 2.5.

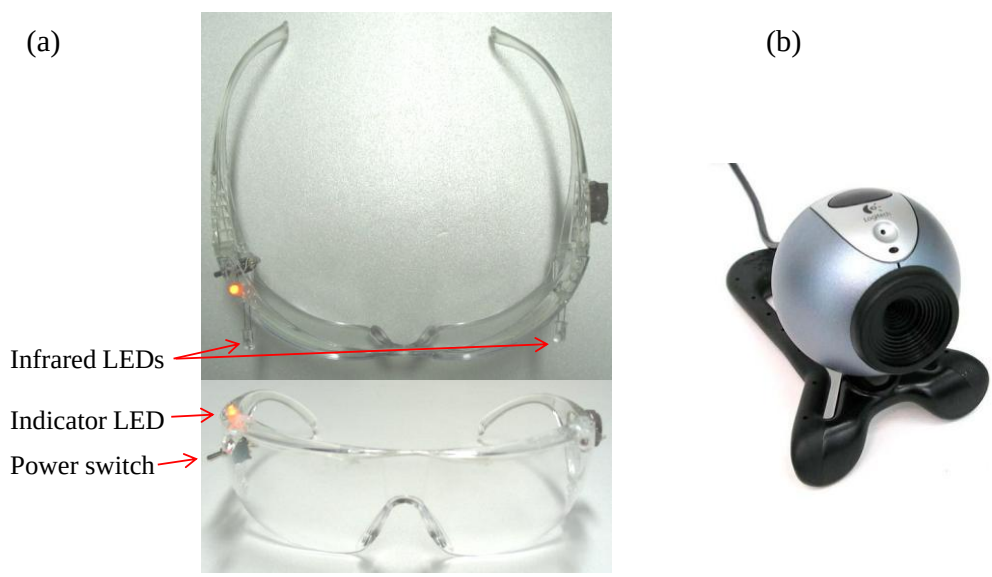

Figure 2.4 (a) A goggle equipped with two infrared LEDs and (b) an infrared camera

modified with a USB camera

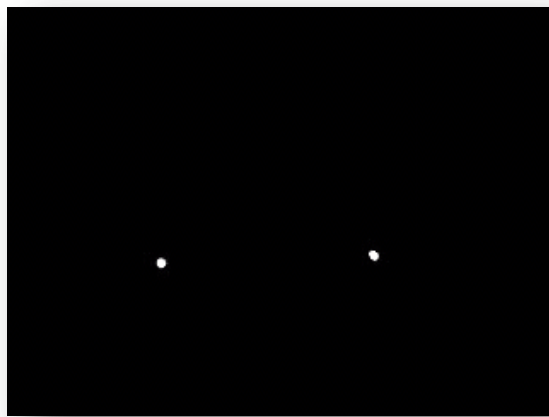

Figure 2.5 An image from the infrared camera. Two white points are infrared LEDs in the goggle.

Table 2.1 Specification of tracking system with infrared LEDs

Infrared Camera	Model	Logitech Quickcam IM
	Resolution	320 x 240
	Frame rate	30 Hz
Infrared LED	IR frequency	940 nm
	Power	50 mW
S/W Environment	Language	C++
	Library	OpenCV 2.1

The viewing angle of the infrared camera is so small that it covers only about 30 degrees horizontally. Therefore, a convex mirror is used to track an omni-directional

observer as shown in Fig. 2.6. The distance between the infrared camera and the convex mirror can be calculated to find the observer positioned in the same plane as the convex mirror.

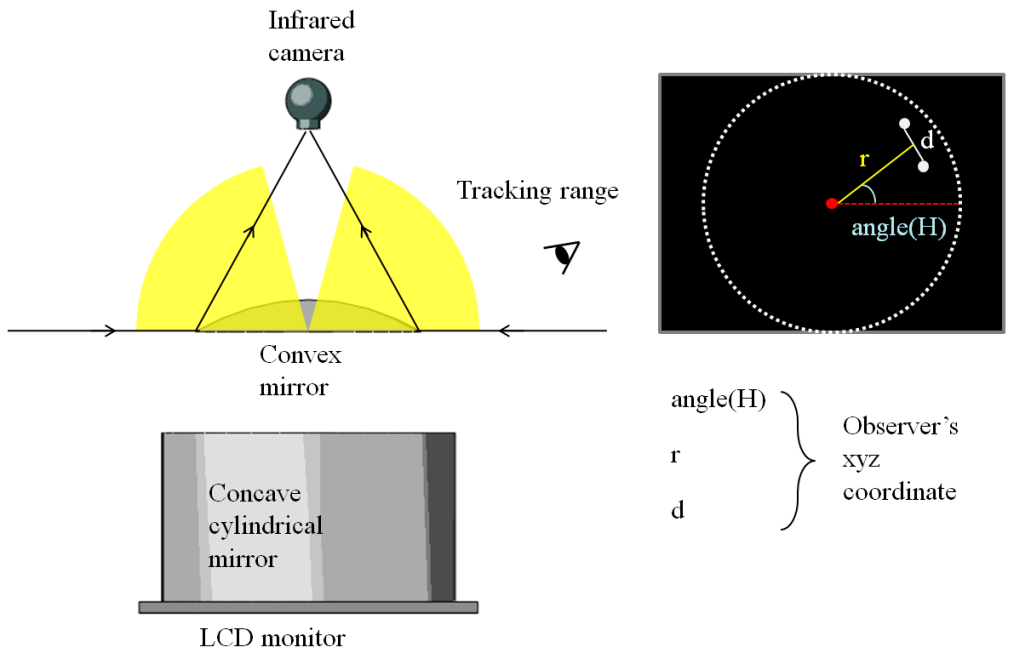

Figure 2.6 Expanded tracking range with a convex mirror and an observer's coordinate parameters

The results from the infrared camera are 2D images with two LED points. For three-dimensional information of the position of the observer, the height of an observer is assumed to be the same as 500mm above the monitor plane.

2.3. Implementation floating display system with tracking technology

The proposed system is composed of a concave cylindrical mirror, a convex mirror, a monitor and tracking camera as shown in Figure 2.7. The cylindrical mirror has a rule to float the images on the LCD monitor to the upper plane of the cylindrical mirror, and to

provide floating images to any direction horizontally around the system. But the cylindrical mirror does not deliver 2D image to viewers without any distortion. The curved surface distorts images on the monitor differently for different positions of observers. For displaying normal images, the distortion should be compensated with calibration.

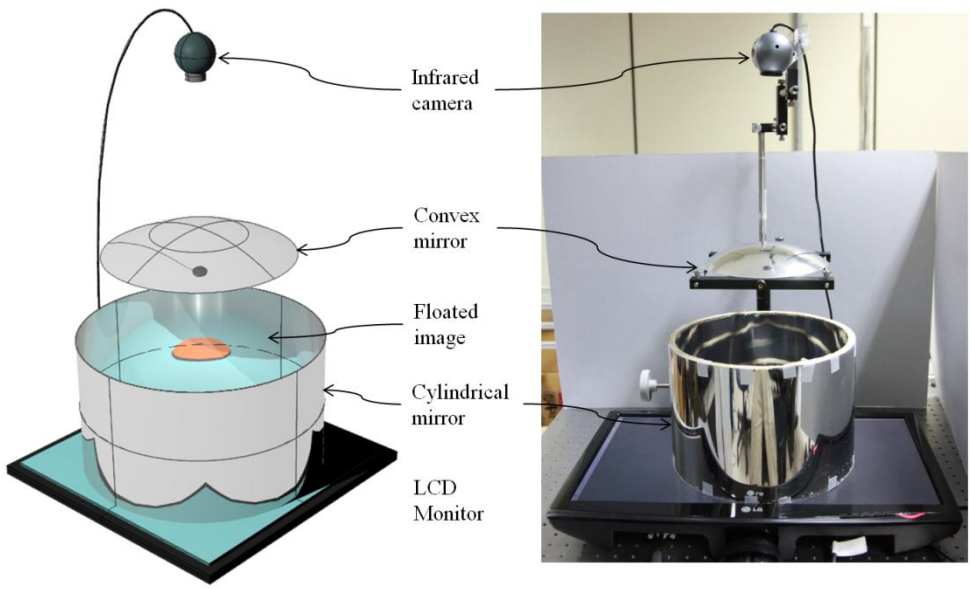

Figure 2.7 The structure of proposed three-dimensional floating display system with a concave cylindrical mirror and tracking technology.

We experimented with optical devices which have specifications as shown in Table 2.2 Experimental specification of components. The cylindrical mirror is made with a reflective film large enough to cover 24 inch LCD monitor. The output resolution of the infrared camera is set to QVGA resolution for tracking in real-time.

Table 2.2 Experimental specification of components

Cylindrical mirror	Radius	145 mm
	Height	200 mm
Convex mirror	Radius	95 mm
	Curvature radius	146 mm
Infrared camera	Resolution	320(H) x 240(V)
	Viewing angle	33˚(H)
	Frame rate	30 Hz
LCD monitor	Resolution	1920(H) x 1080(V)
	Pixel pitch	0.277 mm

Figures 2.8 and 2.9 show mapped sample images for a grid and a teapot object when the position of observer is (-500, 0, 500) and (-350, -350, 500) mm respectively. Two different images in Figures 2.8(b) and 2.9(b) are mapped images for a normal grid image to float as shown in Figures 2.8(a) and 2.9(a) with different positions of observers. Figures 2.8(d) and 2.9(d) show the mapped images for a normal teapot. Images in Figure 2.10 are captured in seven positions with an infrared LED goggle. The z-coordinate means the height from the monitor plane. Since it is possible to recognize horizontal and vertical motion parallax without any change of the height, the z-coordinate is fixed to z = 500 mm. As the observer moves with the same distance from the center of the cylindrical mirror, horizontal motion parallax can be checked. And with the change of the distance from the center of the cylindrical mirror, vertical motion parallax is shown. The reason the shape of the teapot is distorted a little bit is that the mirror does not have exact constant curvature because a flexible mirror film is used.

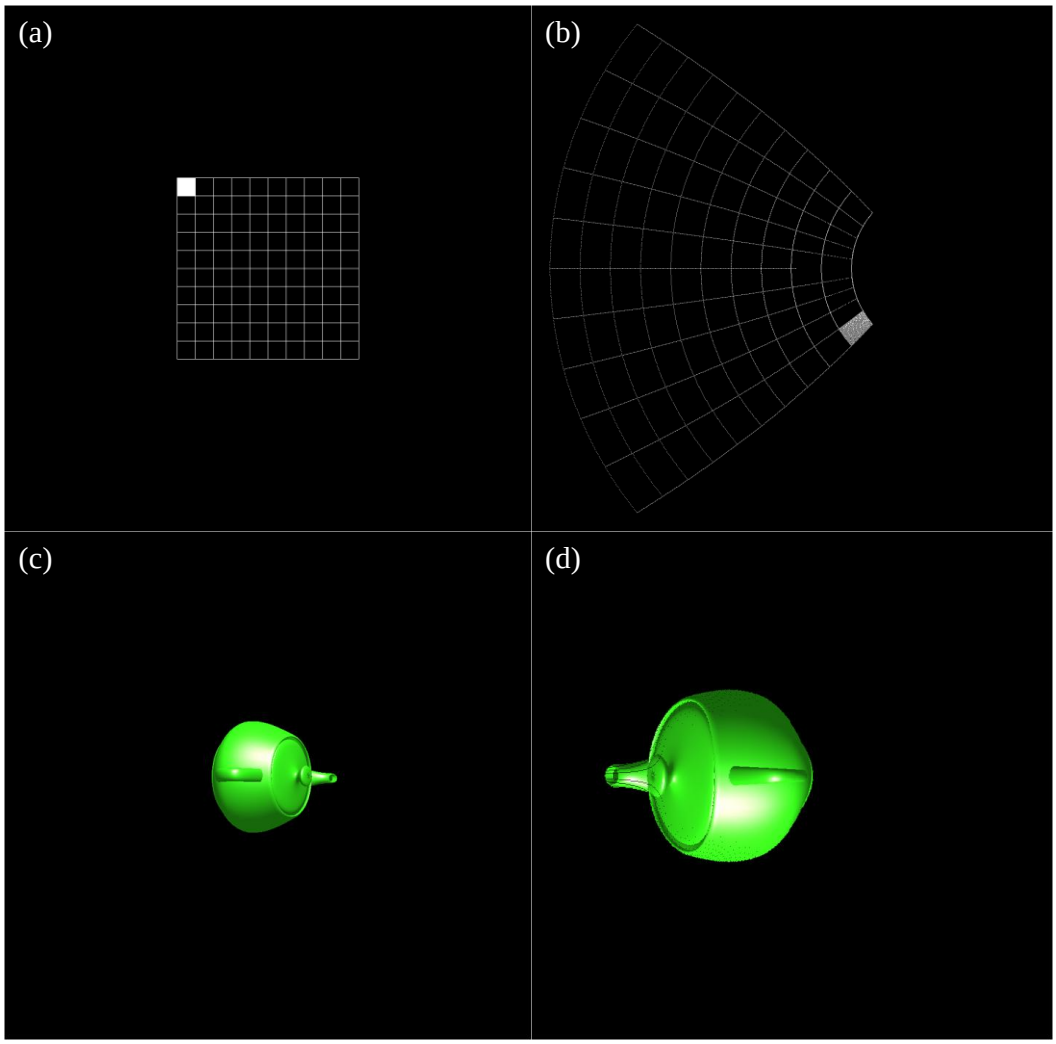

Figure 2.8 When observer 1 is at (-500, 0, 500), (a) original grid, (b) mapped grid, (c) original object image, and (d) mapped object image

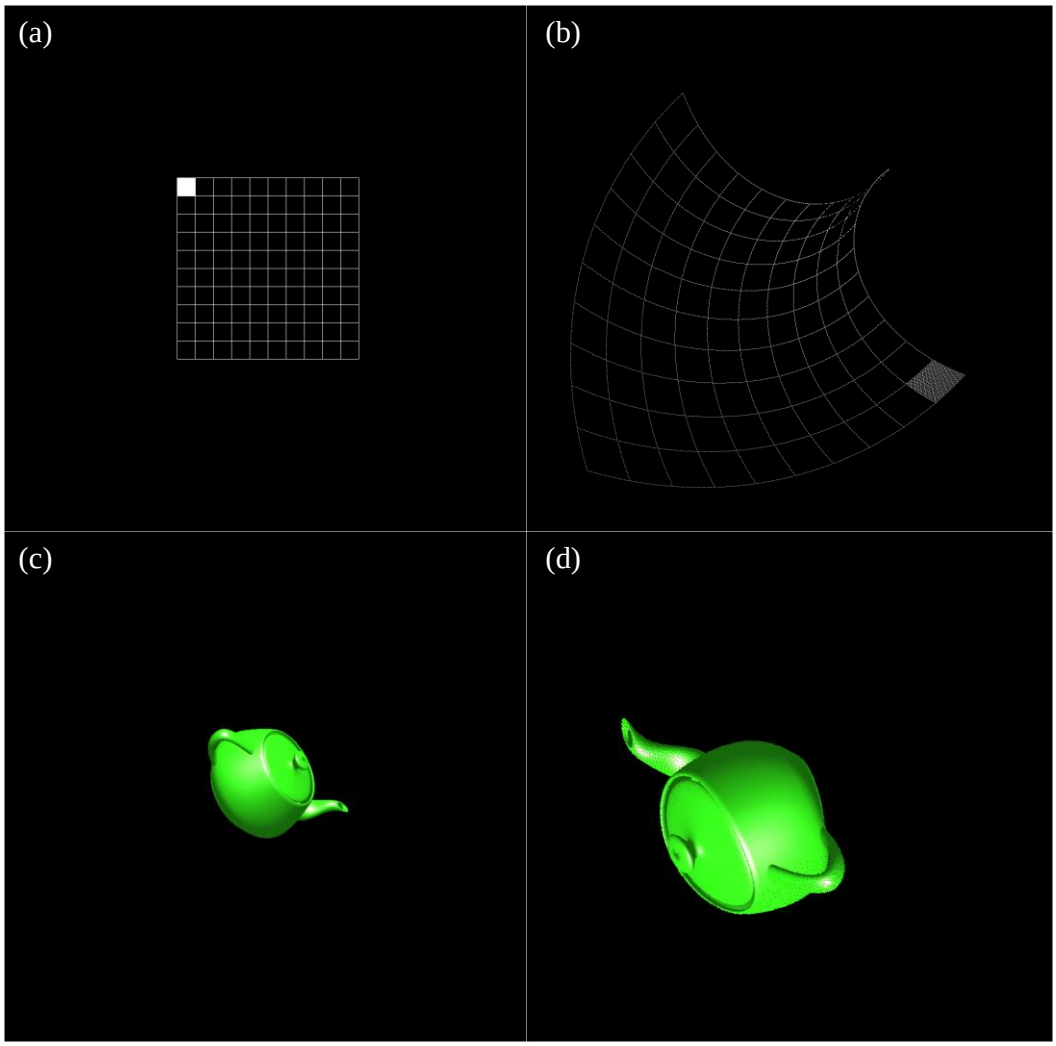

Figure 2.9 When observer 1 is at (-350, -350, 500), (a) original grid, (b) mapped grid, (c) original object image, and (d) mapped object image

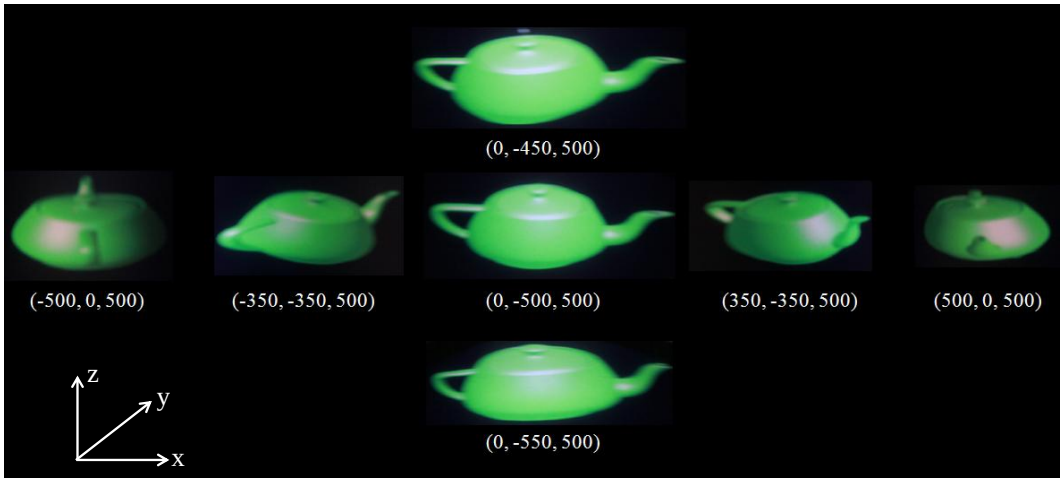

Figure 2.10 Images from various viewpoints. Each coordinate means the position of the observer relatively from the system. (unit : mm)

In this chapter, 3D display system with tracking technology is introduced which can make the use of a cylindrical mirror for providing omni-directional view. Image distortion from a cylindrical mirror is calibrated by image mapping using ray tracking method. This method can be used in other applications which use a cylindrical mirror.

3. Generation of base images for anamorphic volumetric display

Tracking technology has advantages in that the resources in the system can be used for the tracked observer with high efficiency. However, when there are two or more observers, we should use time-sequential or spatial multiplexing method for supporting multiple observers, or assume the situation with only one observer.

In the proposed anamorphic volumetric display system, tracking technique is replaced with time-sequential multiplexing method with a high-speed projector instead of a monitor. Projecting large number of view images using the high speed of a DMD projector, multiple observers in every direction can watch 3D images simultaneously. Chapters 3 and 4 cover image generation part and hardware implementation, respectively.

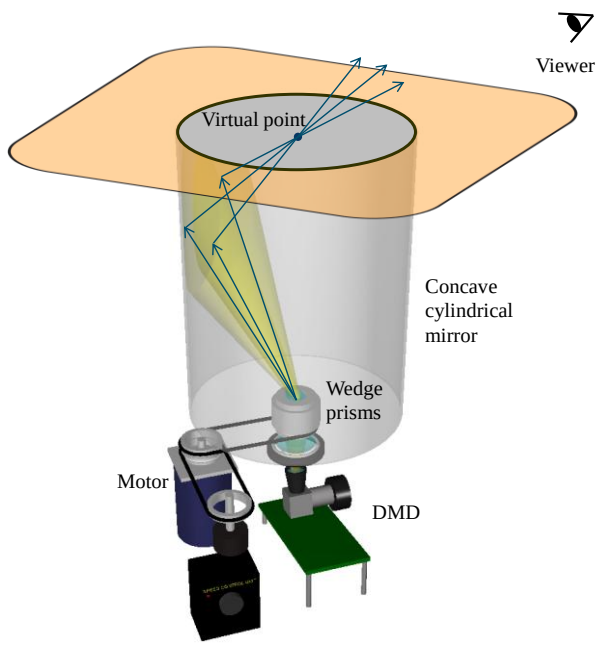

Figure 3.1 The brief schematic of the proposed anamorphic volumetric display system.

Figure 3.1 shows the proposed structure for anamorphic volumetric display system which is composed of a DMD monitor, rotating wedge prisms by a motor, and a cylindrical mirror with an anisotropic diffuser. The further information about each component will be explained in next chapter.

The basic principle of the anamorphic volumetric display system can be understood as following three steps. At first, an image from the projector at a moment is projected to the inner plane of a cylindrical mirror because the optic axis is bended by wedge prisms above the projector. Secondly, there is an anisotropic diffuser attached on the cylindrical mirror surface. The diffuser makes images be diffused only vertically. As a result, when the image reflects on the mirror surface, the image is diffused vertically, and reflected horizontally.

Lastly, when the image is reflected horizontally, every vertical line on the cylindrical mirror is reflected in the different direction. When only one image is projected in a direction, observers can see a narrow vertical line like Figure 3.2. Therefore, to give a directional view image to each direction, it needs composition of images, and calibrate distortions by wedge prisms and the cylindrical mirror.

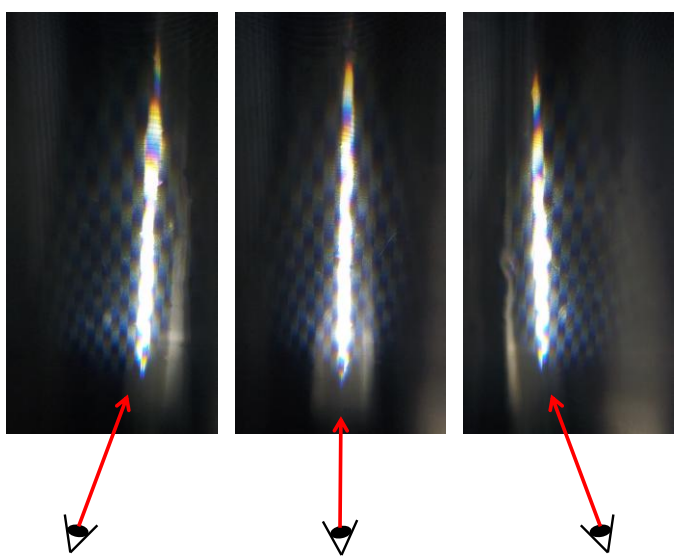

Figure 3.2 Only narrow vertical lines are seen in different directions of observers when an image is projected on the inner surface of the cylindrical mirror through wedge prisms.

To make 3D images with directional view images around the cylindrical mirror, 5 steps are proposed to make base images which are reversely distorted images to calibrate distortions in the system. The 5 steps for base images are as described in the flow chart in Figure 3.3. Each step will be discussed in more detail.

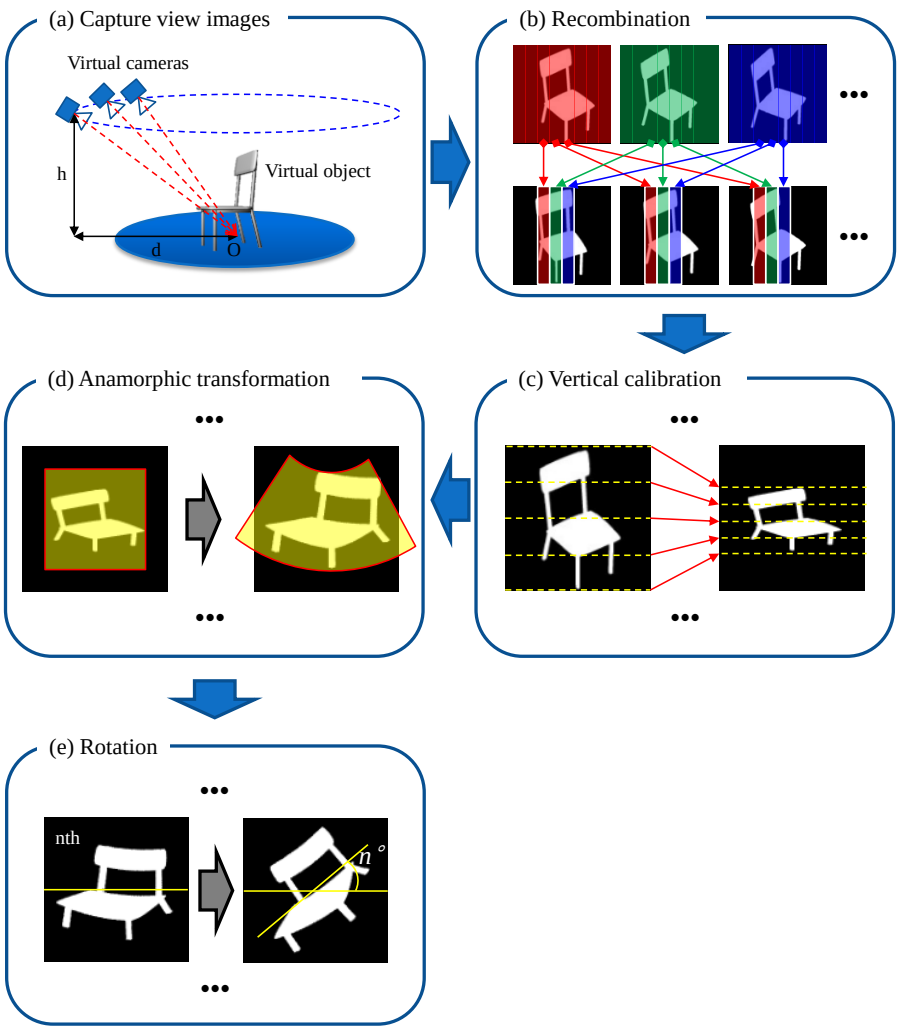

Figure 3.3 Flow chart in generation of base images for anamorphic volumetric display.

3.1. Capturing three-dimensional information by computer graphics

At first, we need view images which are images seen in the observers' positions for displaying 3D images in this system. As shown in Figure 3.1, this system assumes that observers look down images on the center area of the cylindrical mirror. The accurate delivery of view images to observers without distortions is the ultimate goal of this system.

The available number of view images is dependent on the maximum frame rate of the DMD projector. To keep persistence of vision to observers, one rotation with projecting the number of view images should take less than 1/20 seconds. On the other hand, the number of view images decides the density of view images when displaying 3D images. As the number of view images is larger, within the distant range from the cylindrical mirror to satisfy one of depth cues, accommodation can be elongated.

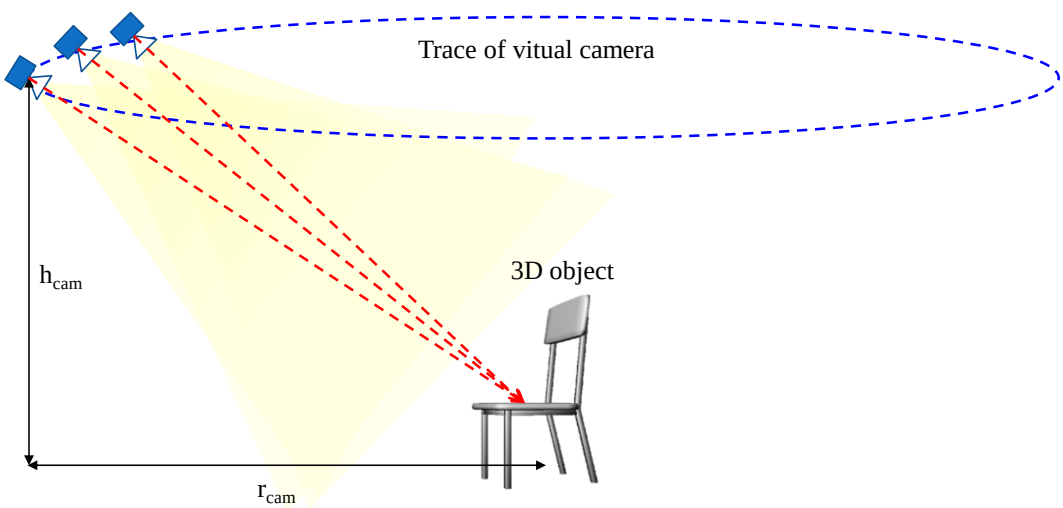

Figure 3.4 The trace of virtual cameras for capturing view images.

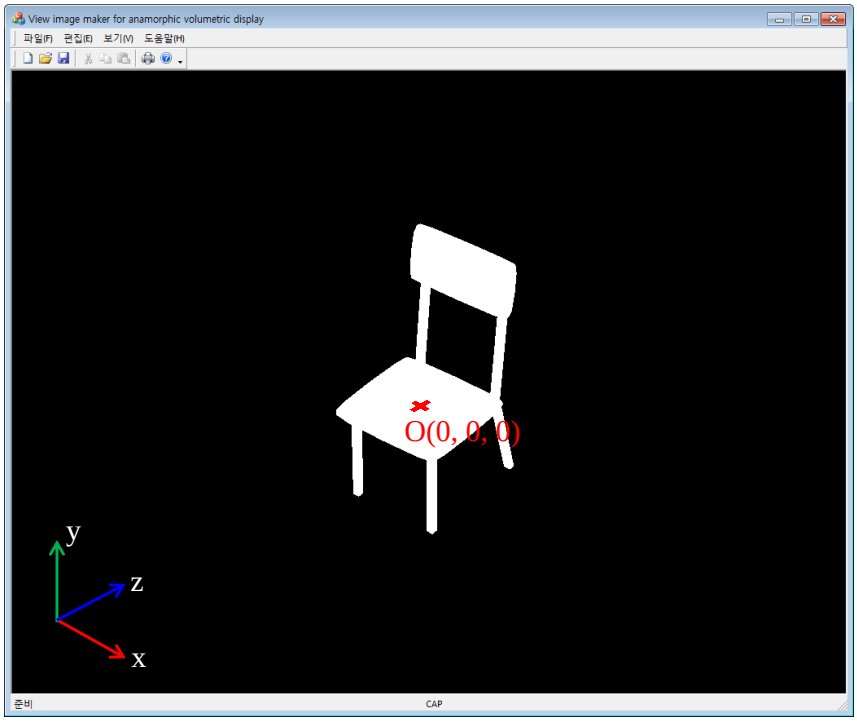

Figure 3.5 The screenshot of the program for capturing view images around the 3D object programmed by OpenGL computer graphic library.

Before capturing real objects, computer graphics library is used to capture view images of a virtual 3D object. Using a customized program for capturing view images in Figure 3.5, arbitrary number of images can be captured. The information of a 3D object model is rendered by a public computer graphic library, OpenGL. In the virtual 3D space, the positions of virtual cameras and the 3D object are as shown in Figure 3.4. The virtual cameras is heading the original point, the 3D object stands in the point. Figure 3.5 also shows the original point and the directions of three axes. As the camera moves to the next position after saving a captured image, the 3D object seems to rotate in the opposite direction. After setting the number of view images as 360, some of the view images captured every 1 degree are shown in Figure 3.6.

Figure 3.6 View images of a 3D object model, chair captured by OpenGL.

3.2. Recombination of view images

The proposed system adopts the anisotropic diffusing to make only horizontal parallax because only horizontal parallax can give better sense of realism of 3D images with better resolution than using both horizontal and vertical parallax. Especially, in the proposed system, viewing zone for watching 3D images is ring-shaped around the system. Therefore the angular scope in horizontal direction is much large than in vertical direction.

For only horizontal parallax, it needs only vertical diffusing on the cylindrical mirror. An anisotropic diffuser is attached on the inner surface of the cylindrical mirror. Without the diffuser, observers cannot watch any view image, but only a bright point per each eye.

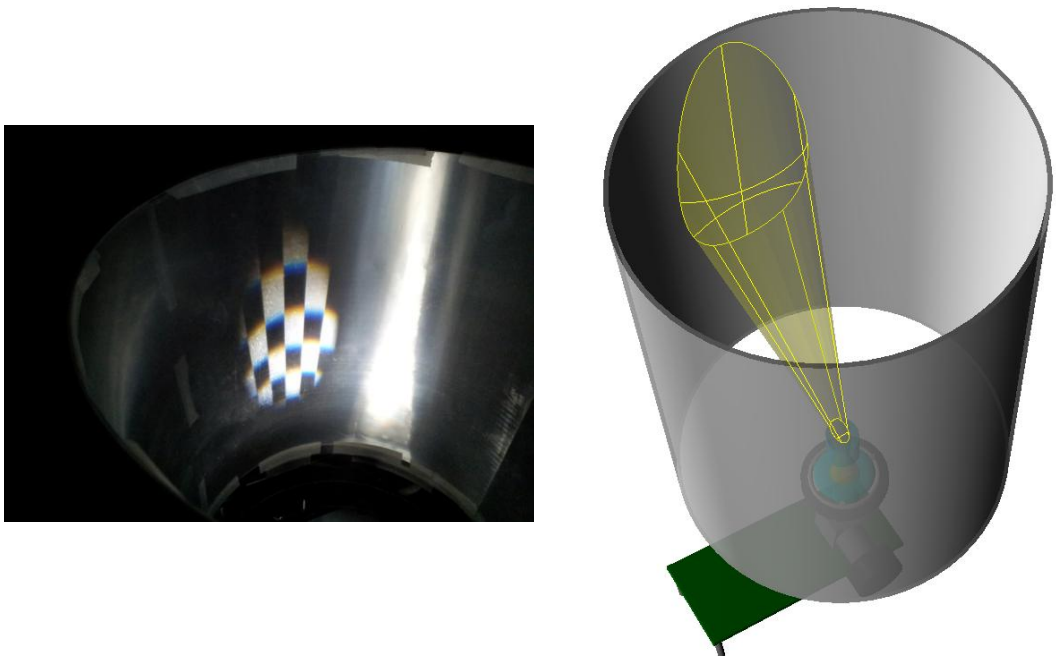

Figure 3.7 A photo (left) and a schematic (right) of the ellipse-shaped projected area on the cylindrical mirror through wedge prisms.

The ellipse-shaped area should not be seen if the anisotropic diffuser attached on the cylindrical mirror is ideal for only vertical diffusing. However, since the diffuser is not ideally good, the brighter vertical line appears when wedge prisms stop as shown in Figure 3.8. The relatively brighter area moves as the observer moves because the brighter line appears when only a vertical bundle of rays from the projector can reach the eye of the observer through the vertical diffuser and the cylindrical mirror. Two bright lines corresponding to two eyes of the observer have different positions on the cylindrical mirror because of horizontally different positions of two eyes. If wedge prism begins to rotate, the position of the brighter area changes as the angle of the prism.

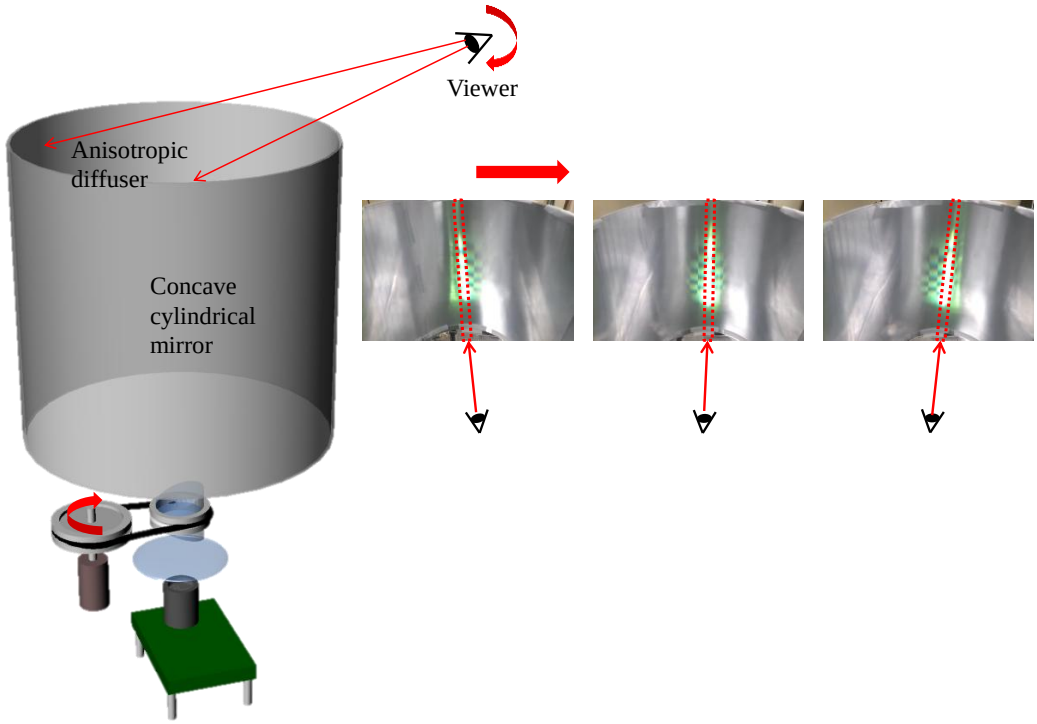

Figure 3.8 The brighter vertical line which moves as the observer moves.

When the wedge prism rotates, the bright area also rotates along the mirror surface. Figure 3.9(a) shows the change of directions as projecting direction rotates. Five bundles of rays in each image in Figure 3.9(a) change their direction as much as the wedge prism rotates. Then, we can combine bundle of rays with the same direction in above five images. Figure 3.9(b) shows view images which are the result of combination of bundle with the same directions. Therefore the inverse combination of view images can be used to make base images. The results of the inverse combination of view images are referred to as the composite images.

To make composite images, view images should be divided with the constant width. The constant width in pixels can be calculated as the arc length corresponding to the angle which is divided 360° by the number of view images. Although the author assumes the bundle of rays go forward in the same direction for convenience, it is not a critical problem because the number of view images is large enough.

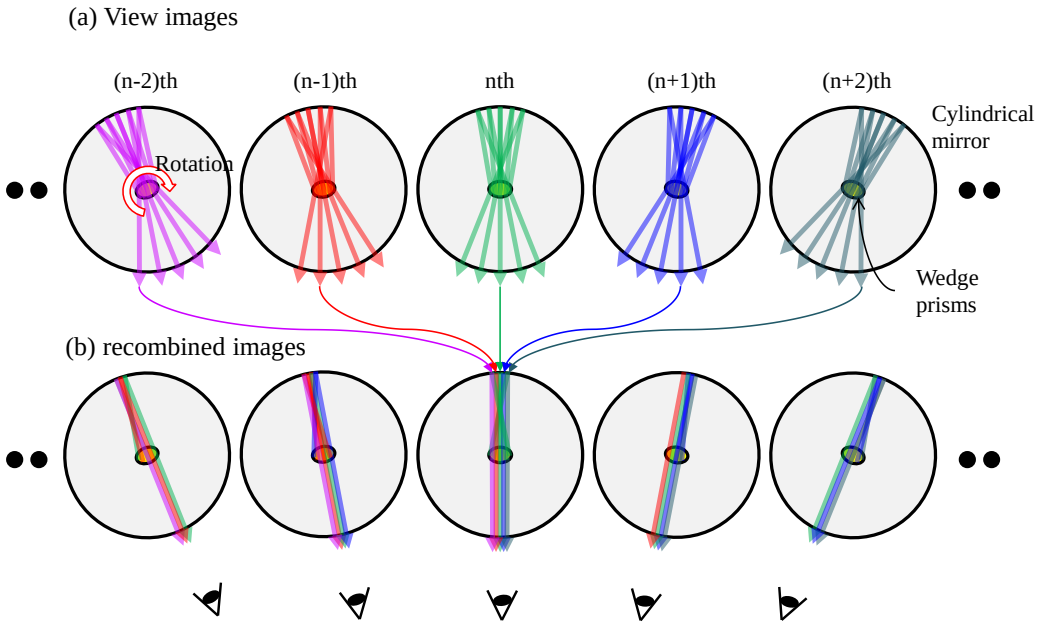

Figure 3.9 Recombined images are made by reflection of view images on a cylindrical mirror. (a) Each view image projects to the specific direction with a diverging angle as the wedge prism rotates. (b) Viewers can watch only recombined images from view images since the rays in view images go forward to different directions by reflection on the curved mirror.

Figure 3.9(a) shows bundles of the rays in view images which are projected through rotating wedge prisms. Those are simplified for convenience with five bundles in each view image. Each bundle reflects on the cylindrical mirror with different direction. As wedge prisms rotate, it can be found that bundles in different view images have the same propagating direction. For this reason, when view images are projected through rotating wedge prisms without any process, viewers can watch only recombined images which are made from combinations of rays from different view images. However, the combinations of projected images by a cylindrical mirror can be used to generate composite images inversely. Composite images mean the images which can show view images to viewers after reflection on the curved mirror.

Composite images can be made by combinations of slice images in view images as described in Figure. 3.10. View images are projected with a diverging angle from a

projector. The width of slice images can be calculated by division of the length of the projected area in pixels with an angle corresponding to each view image.

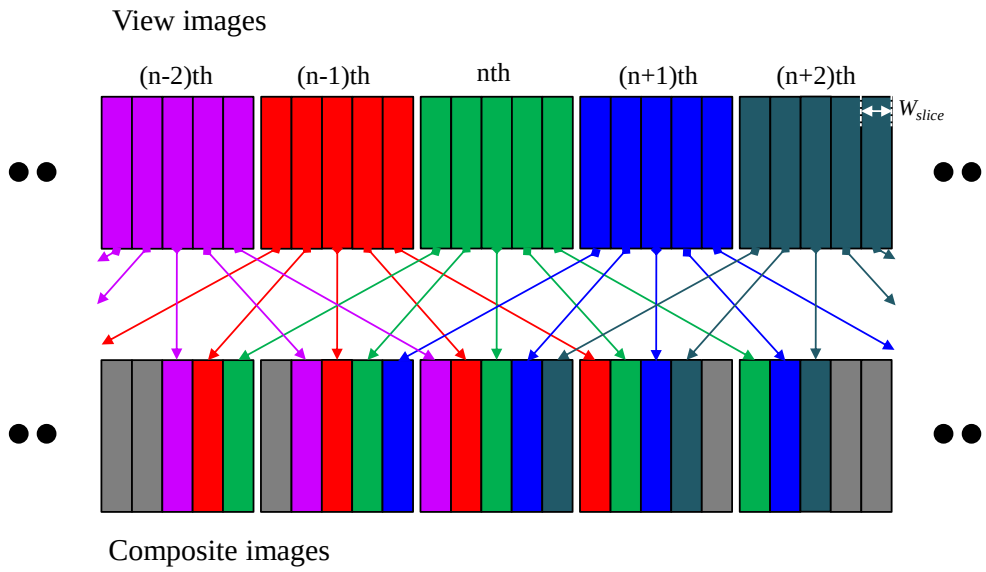

Figure 3.10 Composite images can be made by recombination of slice images from view images. The slice images are divided view images with a slice width, W_{slice} which means the arc length in the cylindrical mirror with the angle of view images.

Projected slice images in a composite image diverge from the wedge prism, and reflect to different directions as shown in Figure 3.11(a). Although the composite images are projected sequentially, slice images can be integrated to view images since the rotating speed of the wedge prism is fast enough.

Composite images can have some discontinuities in the boundary regions with other slice images as shown in Figure. 3.12. However, those discontinuities are removed by combinations of the slice images by reflection on the cylindrical mirror.

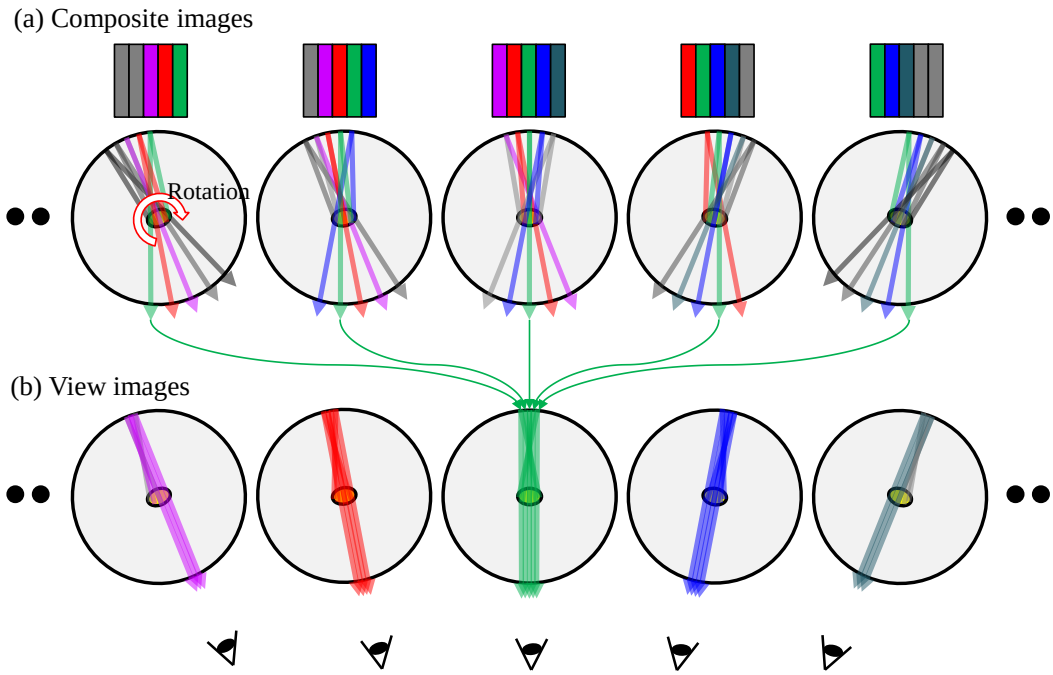

Figure 3.11 (a) Composite images using the different angles on reflections corresponding to the relative positions of rays, (b) displayed view images to the observers in different positions with composite images.

If the number of view images is 360, the angle interval of directional images is 1°. The angle is so small that there are few discontinuities in the most of composite images as shown in Figure. 3.12. These images show sample composite images with discontinuities as the results of the combinations for composite images from view images.

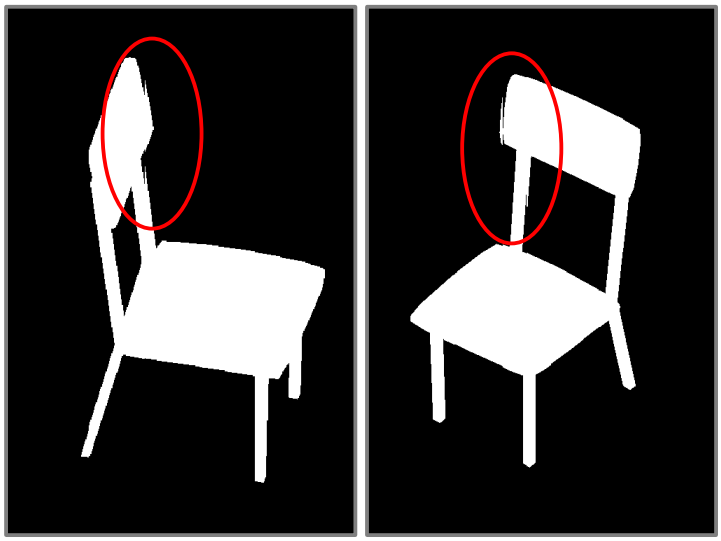

Figure 3.12 Two samples of composite images which have discontinuities (red ellipse areas).

3.3. Vertical calibration of composited images

After the images projected from the projector propagate through the wedge prism which bends the optic axis by refraction in the boundaries of the prisms, the optic axis is not perpendicular to the cylindrical mirror. As a result, the author needs to calibrate different pixel pitches according to the vertical coordinate. For the vertical calibration, some information including vertical projecting angle θ_{ver}, vertical offset angle θ_{offset}, and the number of pixels in a vertical column N_{ver} is required. Figure 3.13 andFigure 3.14 show the angles and N_{ver}.

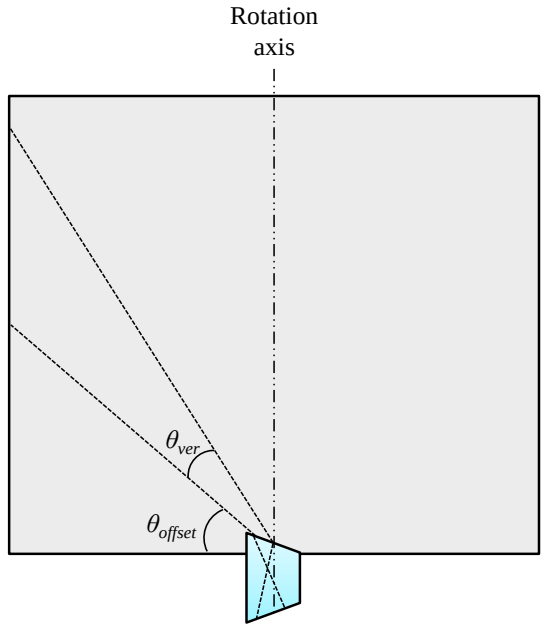

Figure 3.13 Vertical angular range of projecting images from the wedge prism.

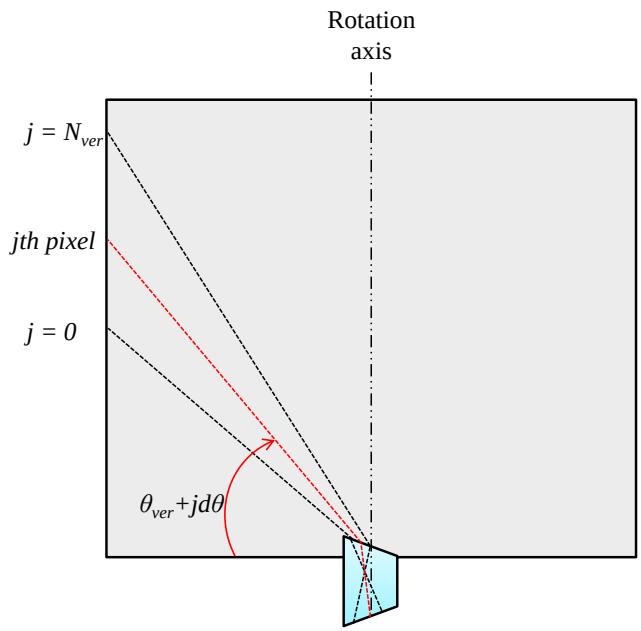

Figure 3.14 The angular position of the j-th pixel in a vertical column of projected images.

To find the pixel pitch of j-th pixel, a simple formula with tangent function is used. In equation (3.1), $d\theta$ is the vertical angle of each pixel. And the pixel pitch of the j-th pixel, $p_{ver,j}$ can be calculated with equation (3.2). In equation (3.2), K is a constant for adjusting the aspect ratio.

$$d\theta = \frac{\theta_{\text{ver}}}{N_{ver}} \tag{3.1}$$

$$\begin{aligned} p_{ver,j} &= K \times \left[\tan(\theta_{offset} + jd\theta) - \tan(\theta_{offset} + (j-1)d\theta) \right] \\ &= K \times \frac{\tan d\theta \left[1 + \tan^2(\theta_{offset} + jd\theta) \right]}{1 + \tan(\theta_{offset} + jd\theta) \tan d\theta} \end{aligned} \tag{3.2}$$

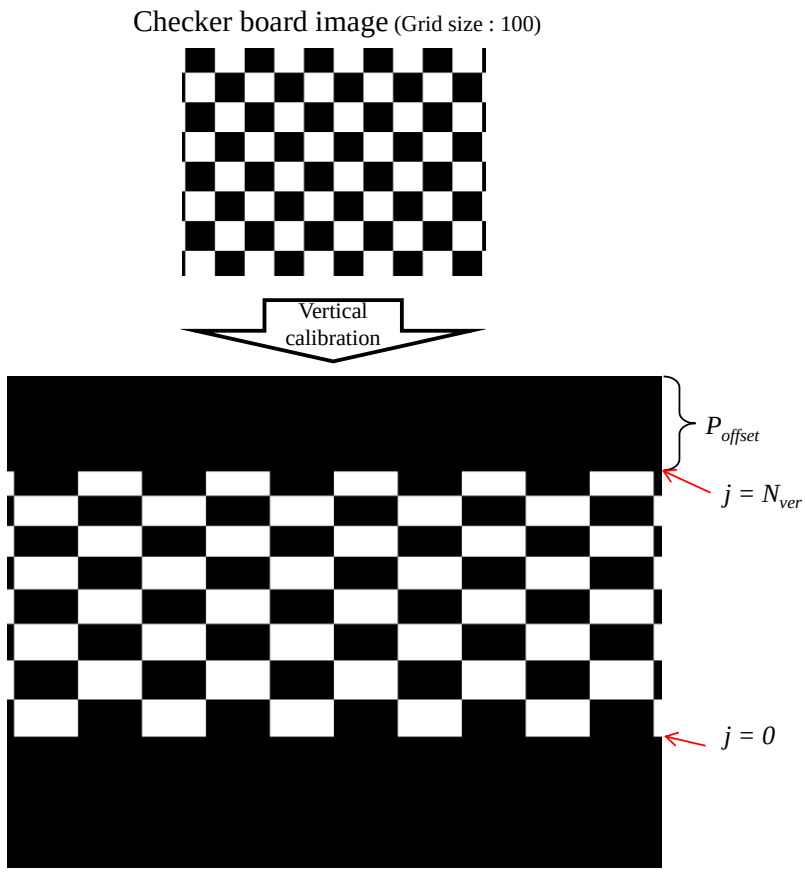

Figure 3.15 A vertically calibrated image with a checker board image whose grid size is 100 pixels. The values of parameters which are used in the calibration are (θ_{ver}, θ_{offset}, K) = (20°, 10°, 700).

The values of parameters like $\theta_{ver,}$ θ_{offset} in vertical calibration are not the same as the measured angle. The reason is that the wedge prism makes the rays deviate with specific angles, and the deviated angles vary in some range as the incident angles of rays are changed. Additionally, it needs more recalibrations after anamorphic transformation for the more accurate setting. Samples of vertical calibrated images using the above equations are shown in Figure 3.16.

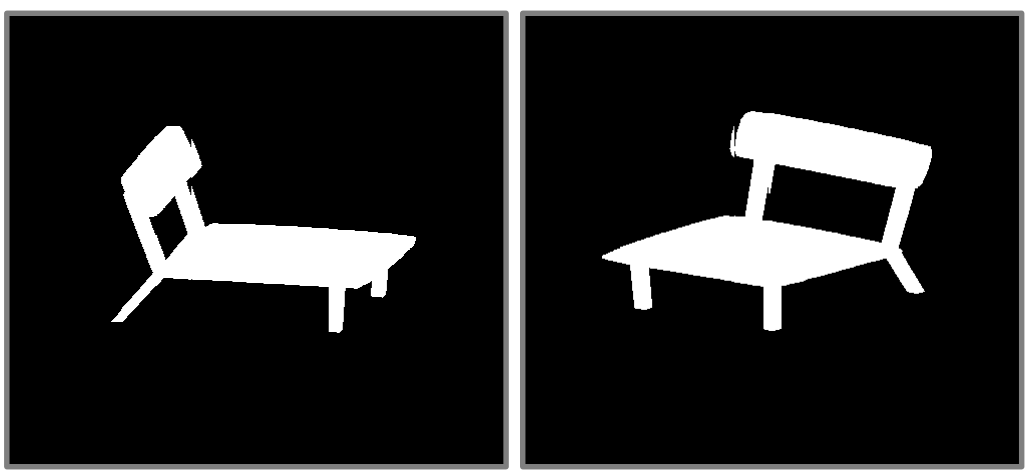

Figure 3.16 Two samples of vertical calibrated images with images in Figure 3.122.

3.4. Anamorphic transformation

Left image in Figure 3.7 is the projected image using a checkerboard image. Watching the image closely, it can be found that each square is distorted with a part of fan-shaped sector. Before calibration, this transition from a square to a fan-shaped sector can be analyzed with transformation between two coordinates as shown in Figure 3.17.

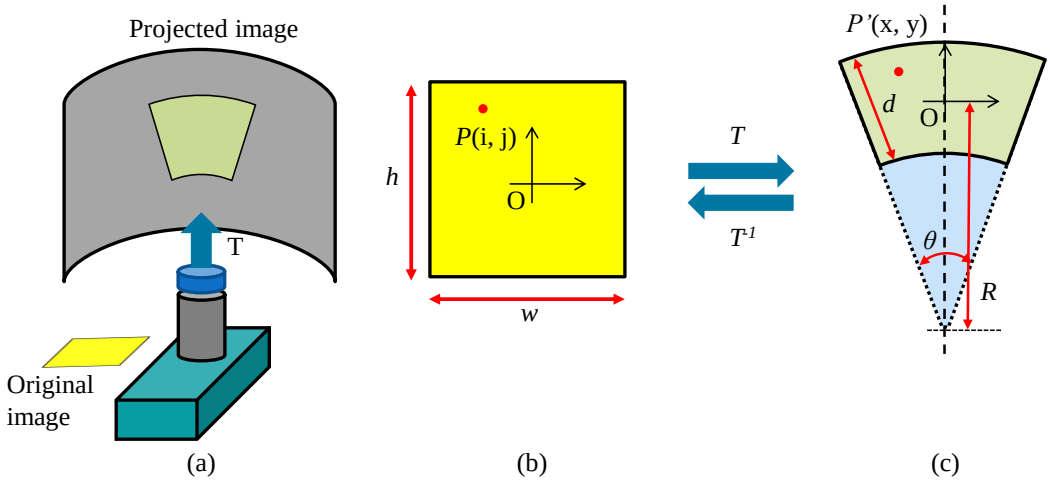

Figure 3.17 Representation of the distortion on a cylindrical mirror by coordinates transformations. (a) Concept of an original image and a projected image, (b) original image in the Cartesian coordinates, (c) projected image in the polar coordinates.

Images from a DMD projector are projected on a cylindrical mirror through the wedge prism with a tilt angle. The distances from the DMD projector to the curved plane of the cylindrical mirror are different depending on the positions of rays. It makes projected images distorted to fan-shaped images like Figure 3.17(a). This distortion can be understood as transformations between two coordinates, the Cartesian and the polar coordinates. Equations (3.3) - (3.6) show the relationship between two coordinates and can be used to calibrate distortion.

$$x = \left(\frac{d}{h}j + R\right)\sin\left(\frac{\theta}{w}i\right) \tag{3.3}$$

$$y = \left(\frac{d}{h}j + R\right)\cos\left(\frac{\theta}{w}i\right) - R \tag{3.4}$$

$$i = \frac{w}{\theta}\tan^{-1}\left(\frac{x}{y+R}\right) \tag{3.5}$$

$$j = \frac{h}{d}\left(\frac{x}{\sin\left(\tan^{-1}\left(\frac{x}{y+R} \right) \right)} - R \right) \tag{3.6}$$

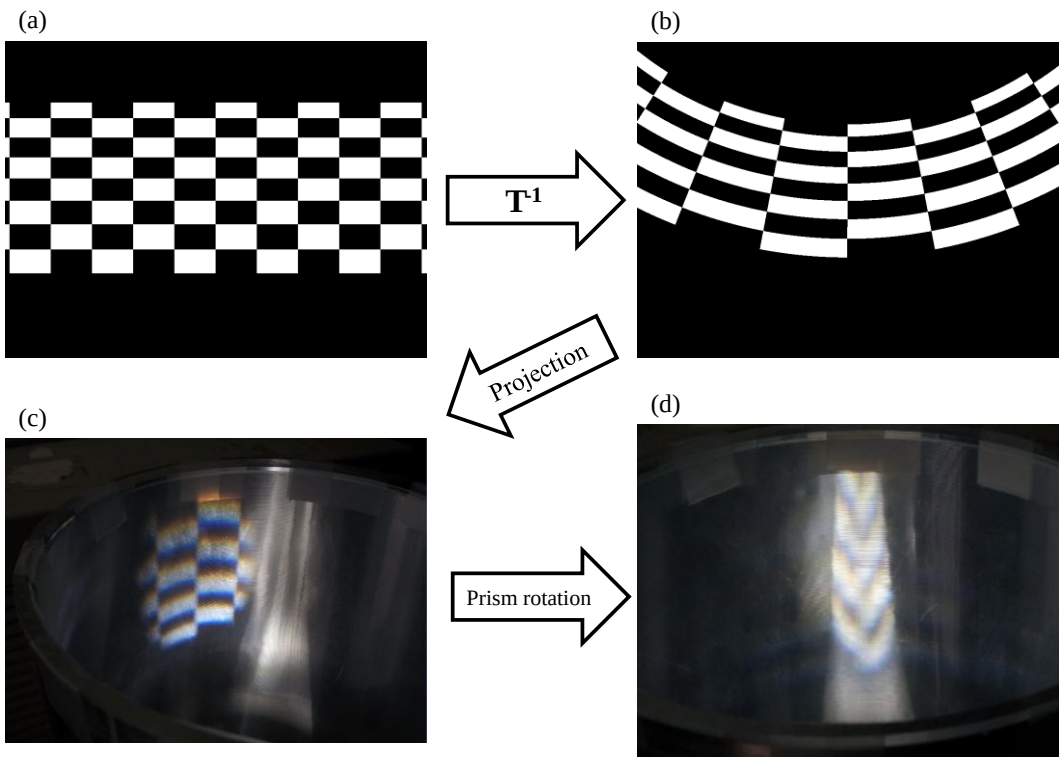

Figure 3.18 Calibration for anamorphic transformations from a cylindrical mirror. (a) Vertically calibrated checker board image, (b) calibrated check pattern image by an inverse anamorphic transformation, (c) a projected image of image (b) with the static wedge prism, (d) a projected image of image (b) with the rotating wedge prisms. (d, R, θ) = (600, 100, 110°)

Figure 3.18 shows a calibration results by coordinate transformations. When a checker board image is projected to a cylindrical mirror, it is distorted as shown in Figure 3.17(a). The distortion is from forward transformation *T* from Figure 3.17(b) to (c). To cancel out

the forward transformation, reverse transformation T^{-1} should be performed as shown in Figure 3.18(b). In this process, it is important to find the values of parameters like d, R, and θ as described in Figure 3.17(c). The values could be measured after measuring distances in distorted fan-shaped check pattern images, and tuned with calibrated results with some iterations with the previous vertical calibration step because anamorphic transformation can also affect the vertical distance with the change of the value of d.

Figure 3.18(c) and (d) show that two cases are different in that observed images can change as the rotation of the wedge prism. The image in Figure 3.18(c) when the wedge prism is static, shows a projected image on the whole projected area on the cylindrical mirror to a viewer. If the cylindrical mirror with an anisotropic diffuser is ideal, the viewer can watch only one slice image in the projected area. However, since the mirror is not ideal, the viewer can see the whole projected area. And when wedge prisms are rotating, a combined image with bright slice images can be seen as shown in Figure 3.18(d). To see the right checker board image on the cylindrical mirror, one more step is needed.

Since this transformations between two coordinates are similar to the transformations in anamorphosis and it is common to transform images reflecting on the curved surface [17], it is refered to as anamorphic transformation or anamorphic images. Two anamorphic images obtained from the anamorphic transformation are shown in Figure 3.19.

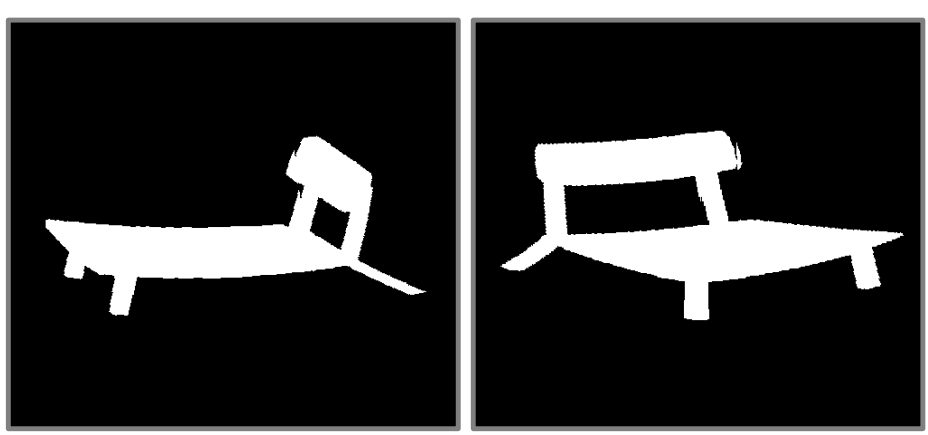

Figure 3.19 Two samples of anamorphic images with coordinates transformation.

3.5. Image rotation by optic axis

From the rotating wedge prism, oblique optic axis from the wedge prism rotates along the cylindrical mirror as shown in Figure 3.20(a). In addition, projected images from the projector rotate against their centers as the position moves along the surface of the cylindrical mirror. The rotation of images can be easily calibrated with the inverse rotation of images.

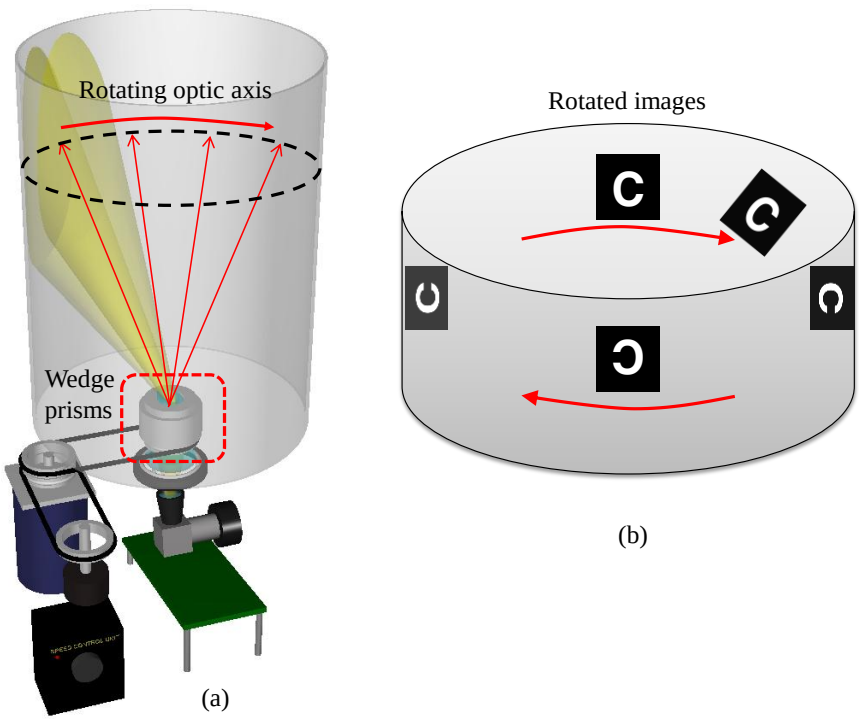

Figure 3.20 Rotation of projected images with rotation of optic axis.

At this moment, the synchronization between the rotating wedge prism and the DMD projector is significant to provide a static image volume. In my system, a rotary encoder which can generate PWM (Pulse Width Modulation) signals is used to send a trigger signal to the DMD controller board. Without the synchronization, 3D image can be distorted with variable speed of the motor or be rotated with an irregular speed. Figure

3.21 shows the calibrated image volume with five steps for the image volume. The images are rotating in the speed synchronized with the motor.

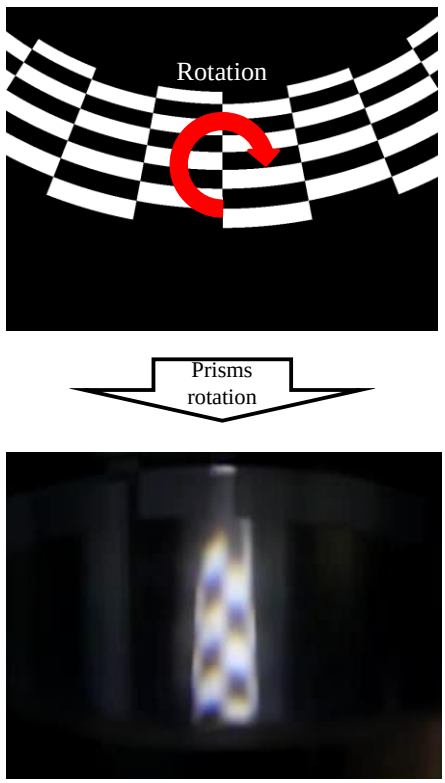

Figure 3.21 Rotation of inversely anamorphic transformed images synchronized with the rotation of wedge prism can generate the image volume with a normal checker board pattern.

All of five steps are discussed in order. Since each process has to deal large number of images, the same as the number of view images, parallel processing should be implemented for real-time applications. Some sample images in intermediate processes are shown in Figure 3.22. The rotated images after the 5th step are the final base images for projection. The experimental results will be shown in next chapter.

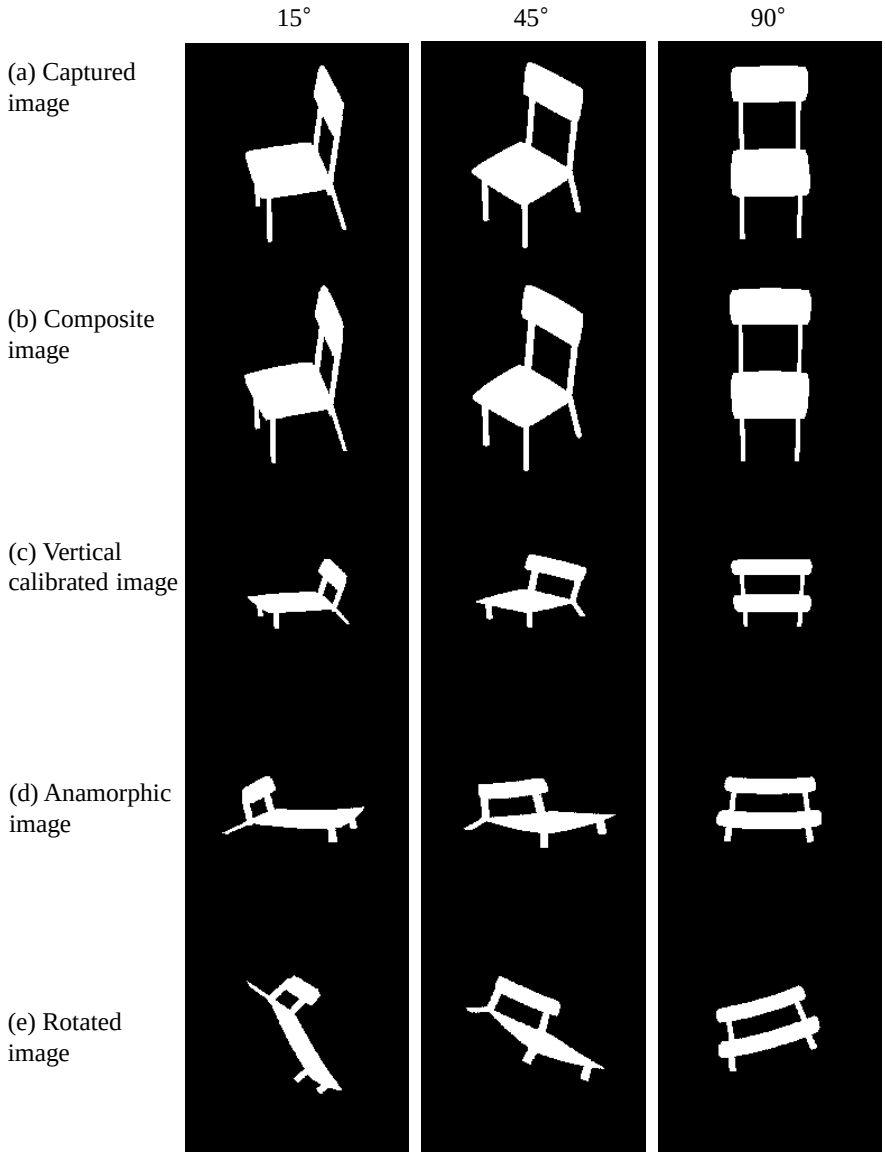

Figure 3.22 Sample intermediate images at three angles for base images which are the rotated images.

3.6. Capturing three-dimensional information of real objects

Figure 3.23 shows a fundamental experimental setup to capture a real object with a CCD camera. To capture view images around the object, a rotational motor stage is used. The CCD camera captures images every time the stage rotates 1° in the direction to the center of the object.

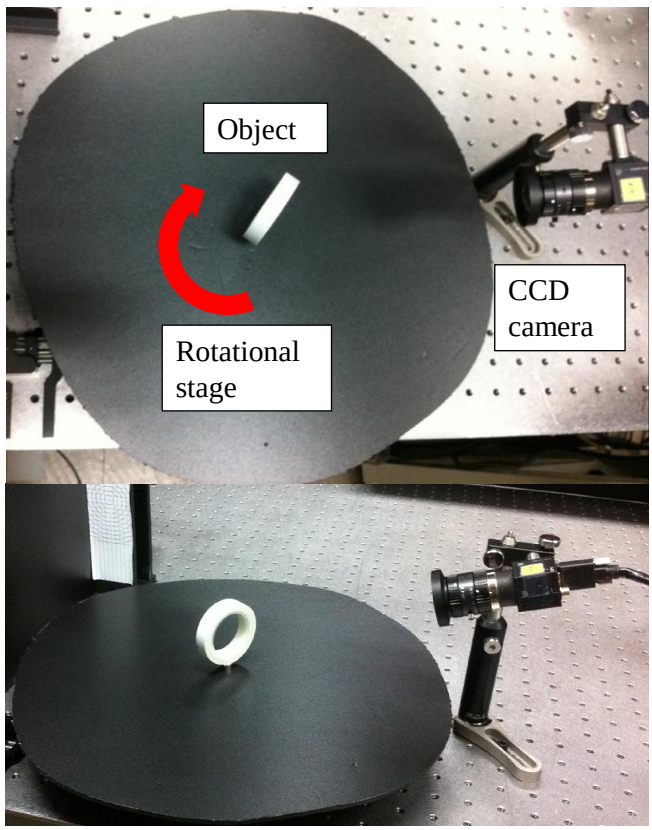

Figure 3.23 Experimental setup for capturing real objects

Since it is important to adjust the original point of the rotation, a specific area in each photo is cropped to black images, and binarized with a proper threshold value because the DMD projector uses only binary data for the highest speed in this system. The sample images in the intermediate processes are shown in Figure 3.24.

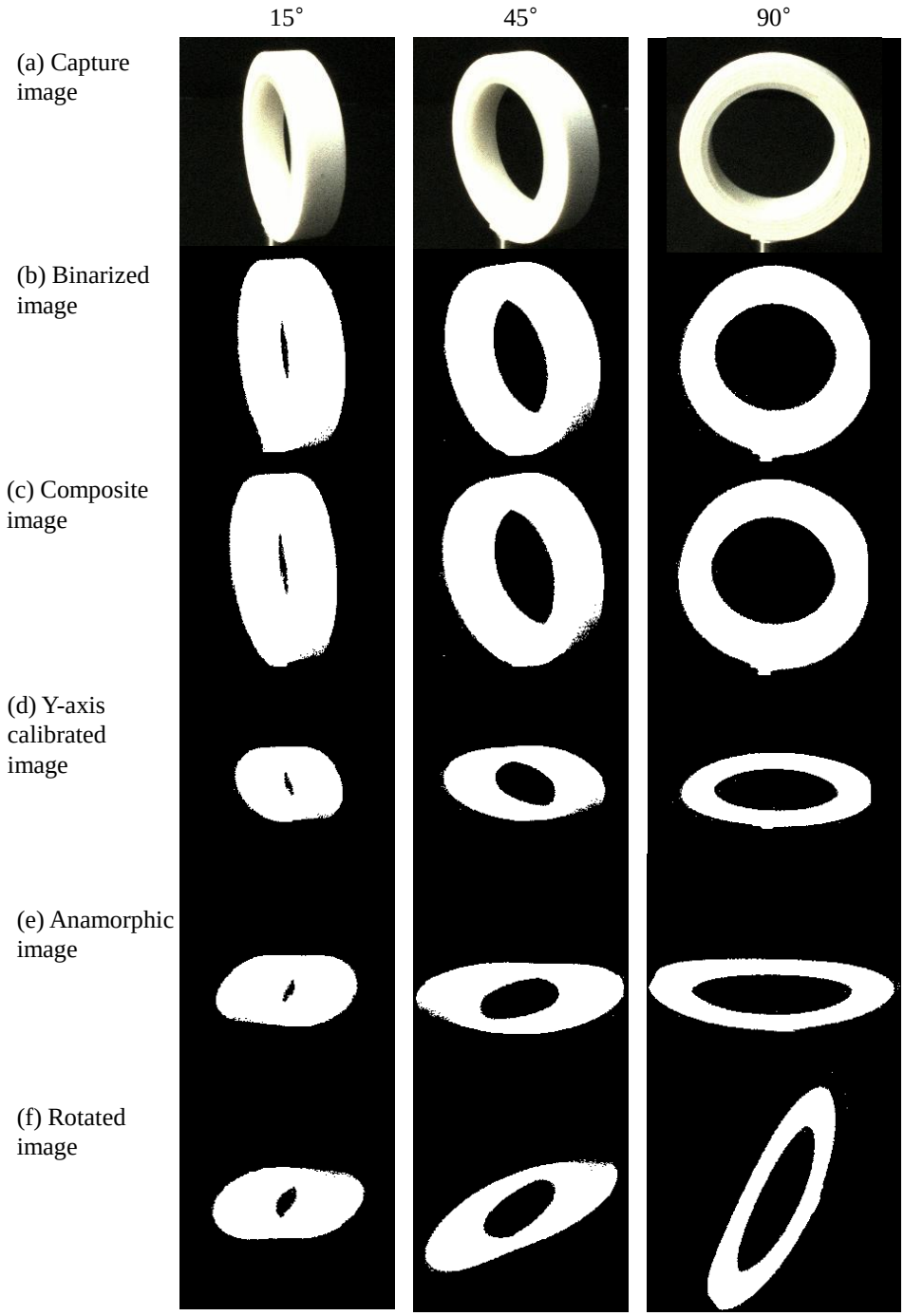

Figure 3.24 Sample intermediate images at three angles using images captured from a real object, circular tape.

4. Implementation of anamorphic volumetric display

This chapter covers further information of main hardware components in the proposed anamorphic volumetric display system. The main components are a high-speed DMD projector, a rotating wedge prism, and a cylindrical mirror with an anisotropic diffuser as shown in Figure 4.1.

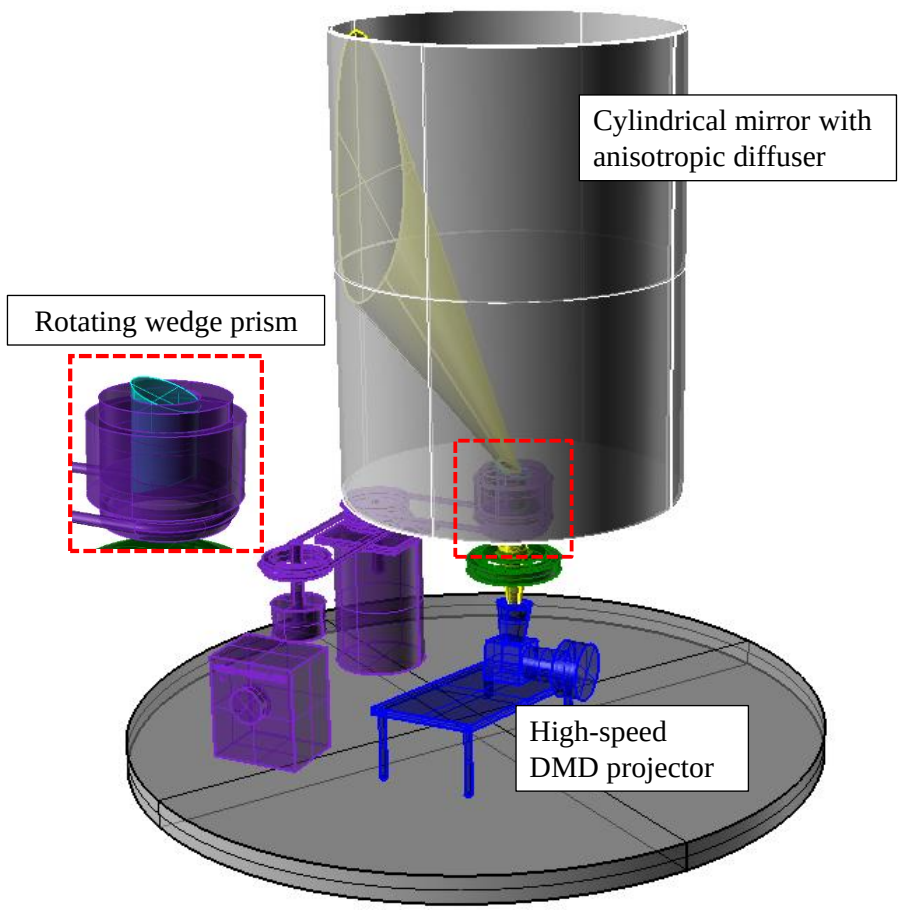

Figure 4.1 Three main components of anamorphic volumetric display system

A similar structure with two relay mirrors can be shown in [28]. There are differences in which the system uses two rotating mirrors instead of wedge prism, and does not use a cylindrical mirror with a cylindrically curved anisotropic diffuser but uses a planar anisotropic diffuser on a cylinder. It means that the system can have less color dispersion on the vertical axis, and have bigger moving parts which include two planar mirrors and the planar diffuser. Wedge prisms in the proposed system can reduce the number of rotating components.

4.1. High-speed DMD projector

High-speed projector is one of the easiest ways to display relatively large information with a large amount of bandwidth in display systems because the frame rate of the high-speed projectors using DMD chipsets is higher than 10,000 fps even though with binary images are used. Time-sequential multiplexing with the high-speed projector can be useful to reduce the number of displaying devices like projectors especially in the case of volumetric display systems which need much more information than general two-dimensional display systems.

For compact volume of the anamorphic volumetric display system, only a high-speed projector is considered. In the specification of the high-speed projector, resolution and frame-rate are critical to decide the capability of the system. As a matter of fact, there are not many kinds of commercialized high-speed projectors in the market. The most popular type of high-speed projectors is a DMD projector with high-speed data processing module.

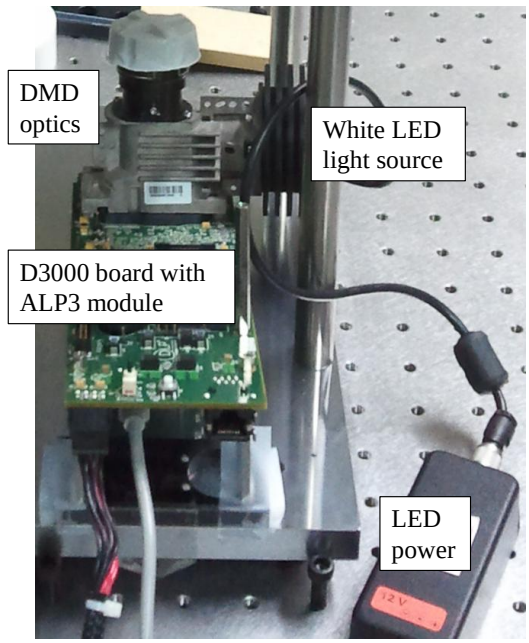

Figure 4.2. The organization of a DMD projector with ALP high-speed module.

In the aspect of the proposed system, two parameters have to be considered to decide the specification of projector. They are the number of view images around the cylindrical mirror N_v and the frame-rate of each view image f_v. To make three-dimensional images using time-multiplexing method, the frame-rate should be higher than about 20 fps to give persistence of vision to observers. It is certain that the larger number of view images is better than the smaller one. Dense view images around the cylindrical mirror can reconstruct more natural and continuous images to observers. However, if the observers are distant less than 1 meter from the cylindrical mirror, 360 view images are enough to make continuous views to observers. The more details about the number of view images will be discussed in Chapter 5.

To summarize of the necessary specification of the projector in the proposed system, one is the higher frame rate than 10,800 fps for 30 fps per each view, and the other is whether it can be synchronized with motor speed. In the proposed system, Texas Instrument Discovery 3000 starter kit with ALP-3 high speed module developed by ViALUX is used.

The basic specification of the projector and high speed module is shown in Table 4.1.

Table 4.1 The specification of a high-speed DMD projector

DMD features	Resolution	1024 x 768
	Size	0.7 inch
	Mirror pitch	13.68 mm
	Fill factor	85%
	Trigger in	Yes
ALP-3 module features	Max frame rate (1bit pixel)	13,333 fps
	ALP-3 API language	C++
	DDR RAM	1 Gbit

As the specification of the projector, the maximum frame rate using binary images is more than 10,800 fps. Therefore, 360 view images can be projected every 1/30 second with a trigger input signal.

Figure 4.3 shows the screenshot of a program for image loading programmed by ALP-3 application program interface (API). As described in the figure, basically, image loading and projection of arbitrary numbers of images can be controlled by this program, and the frame rate and the use of trigger input can also be modified.

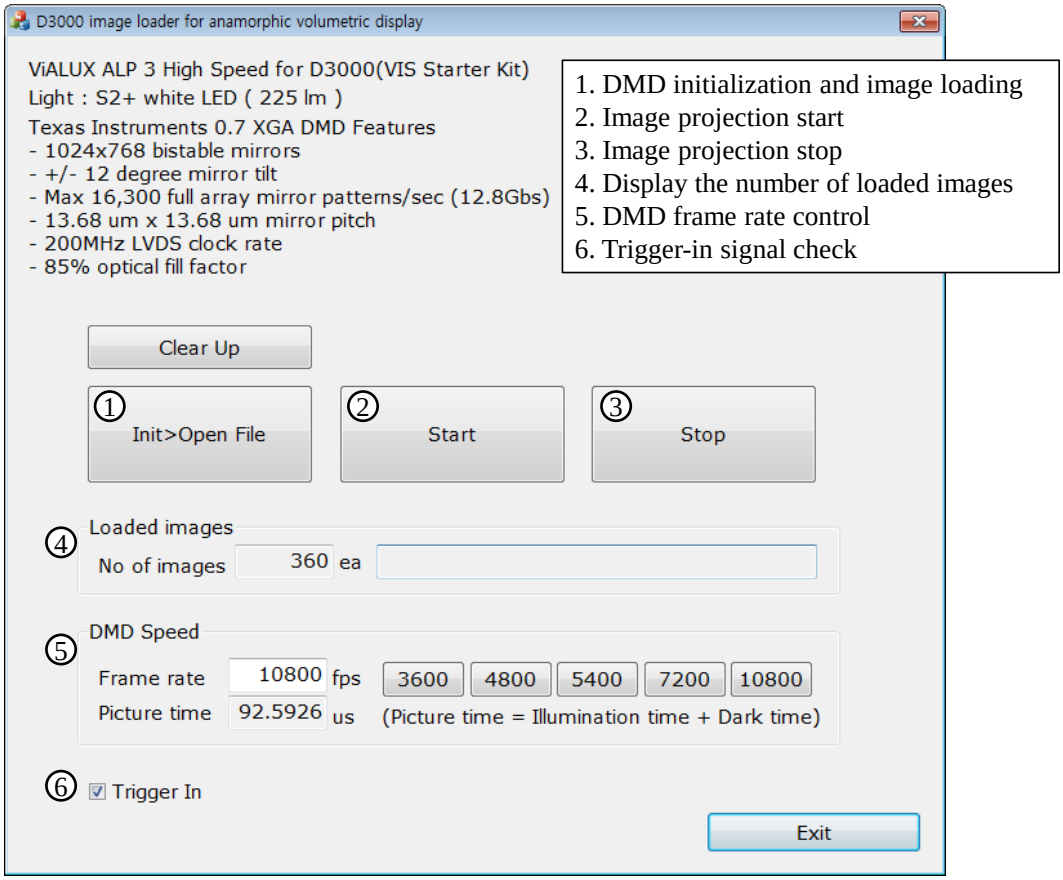

Figure 4.3 A screenshot of a program for image loading programmed by ALP-3 API.

4.2. Spinning wedge prism synchronized with projector

The definition of wedge prism is a prism with a shallow angle between its input and output surfaces [29]. In other words, a wedge prism has different thickness along a direction, which makes the optic axis of input plane deviate with a specific angle as described in Figure 4.4. The refraction through the wedge prism induces deviation of the optic axis. Figure 4.4(a) shows the wedge prism which is used in the proposed system. The diameter of the wedge prism is 25.0 mm. Figure 4.4(b) and (c) are images in two cases without and with a wedge prism captured by a camera heading the same position on an optical table.

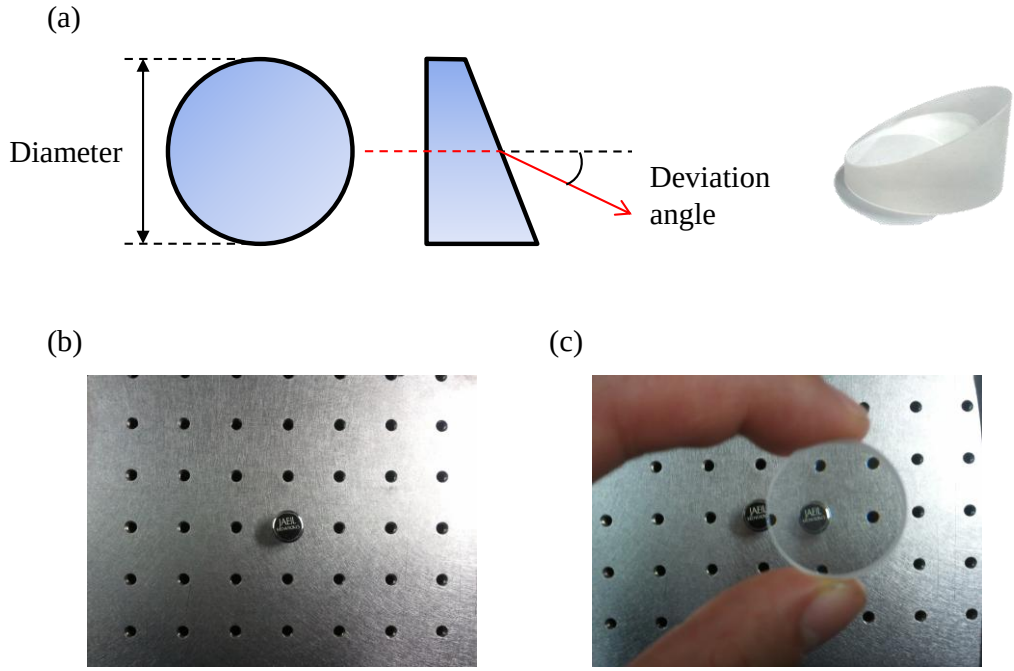

Figure 4.4. (a) shape of the wedge prism which is used in the proposed system, (b) and (c) two images without and with a wedge prism on an optical table.

The rays from a DMD projector bend their directions to outward direction of a cylindrical mirror by a wedge prism. Those rays reflect on the mirror and converge at the center area of the mirror to form volumetric images. In this moment, the deviation angle is important to viewing region of observers. As the angle is larger, the observers can watch images at lower angle. The deviation angle with a wedge prism which is used in the proposed system is 15°. In order to get larger deviation angle, two wedge prisms are attached each other as shown Figure 4.5(a). Attachment of two prisms on the same plane made the angle of 33°, more than two times of its own deviation angle.

Figure 4.5(b) shows the vertical angular range for projection on the cylindrical mirror θ_{ver} and offset angle of the range θ_{off}. The projected images from the wedge prism are elliptic, and their vertical maximum distance in pixel is about 560 pixels. And θ_{ver} and θ_{off} are 23.5°, 44.5°, respectively.

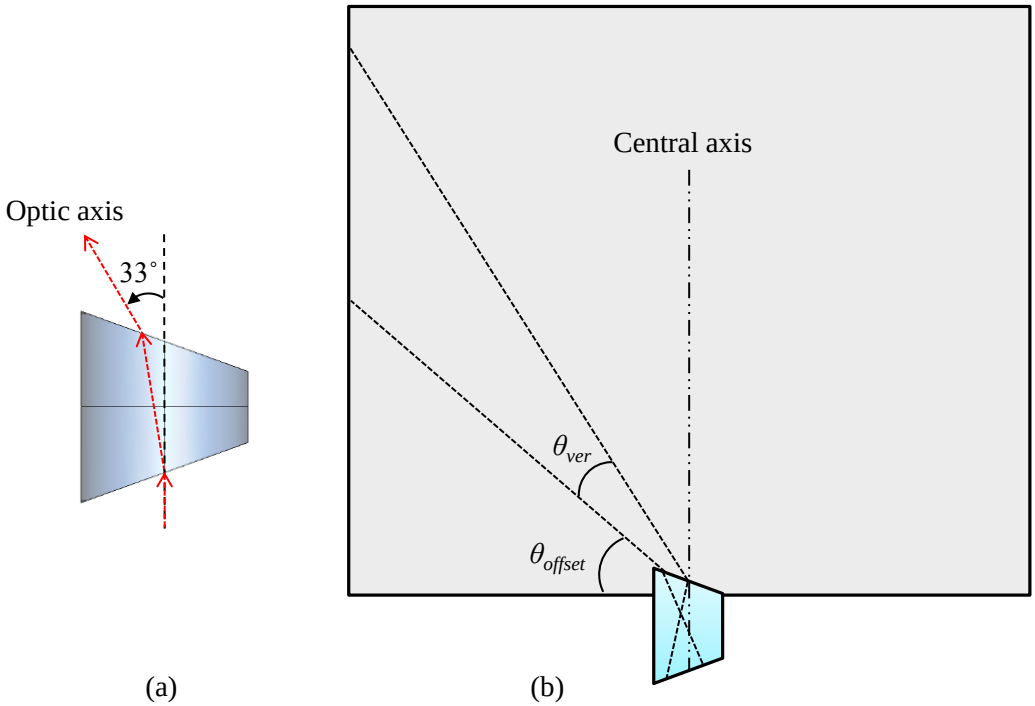

Figure 4.5. (a) wedge prisms attached vertically symmetrically, (b) vertical range of projection angle from the combined wedge prism and offset angle from the bottom plane.

For the rotation of the wedge prism with the center axis of those, the combined prism is fixed with an element which has a hole and tied with a rubber belt connected to a motor as shown in Figure 4.6. The torque for rotation is transferred to the prism by a rubber belt. This structure is designed for the minimization of vibration by the rotation with covering most of the side of the prism with a fixed element. Figure 4.7 shows the projected images with the angle deviated from the wedge prism with the stopped rotation.

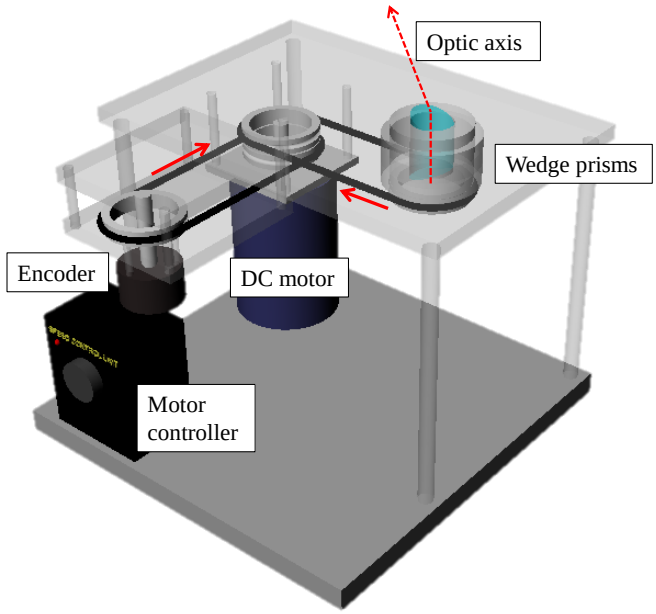

Figure 4.6 A schematic for the rotation of the combined wedge prism by a motor and its controller.

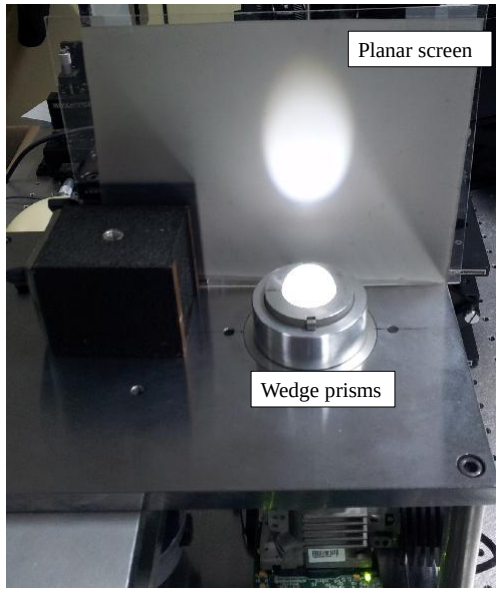

Figure 4.7 Deviated projected images through the combined wedge prism on a vertical planar screen.

4.3. Concave cylindrical mirror and anisotropic diffuser

In the author's system, a concave cylindrical mirror is made by a transparent acrylic cylinder with attachment of reflective films on the inner surface of the cylinder as shown in Figure 4.8. The author made two cylindrical mirrors with different sizes. The inner diameter of one is 254 mm and the height 370 mm. In the case of the other one, the inner diameter is 144 mm, and the height 200 mm.

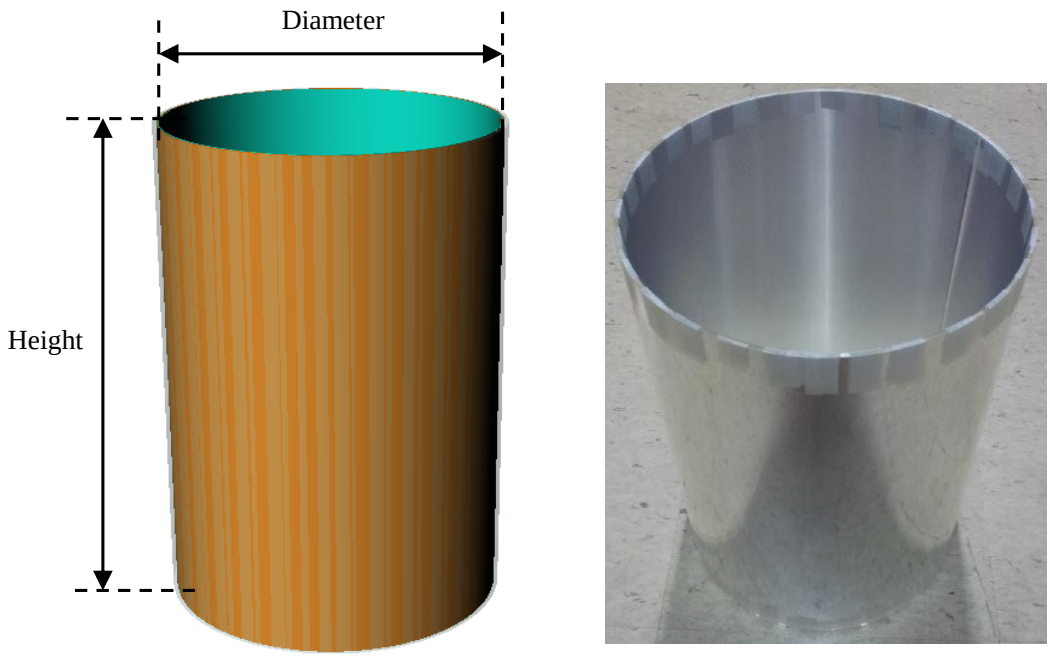

Figure 4.8 The cylindrical mirror made by a transparent acrylic cylinder, reflective films, and an anisotropic diffuser.

In addition, for only vertical diffusing on the inner surface of the cylindrical mirror, an anisotropic diffuser is attached along the horizontal direction. As the anisotropic diffuser, flexible lenticular films whose pitch density are 100 LPI (Line Per Inch) are used. In other words, the order of attachment on the inner surface of the cylinder is described in Figure 4.9. The projected images from wedge prisms are reflected on the surface of the reflective film and diffused in only vertical direction as shown in Figure 4.10. The red fan

shape in Figure 4.10 means the diffusing range by the anisotropic diffuser. If the vertical diffusing range is enough, observers can watch the whole surface of the reflected area of projected images.

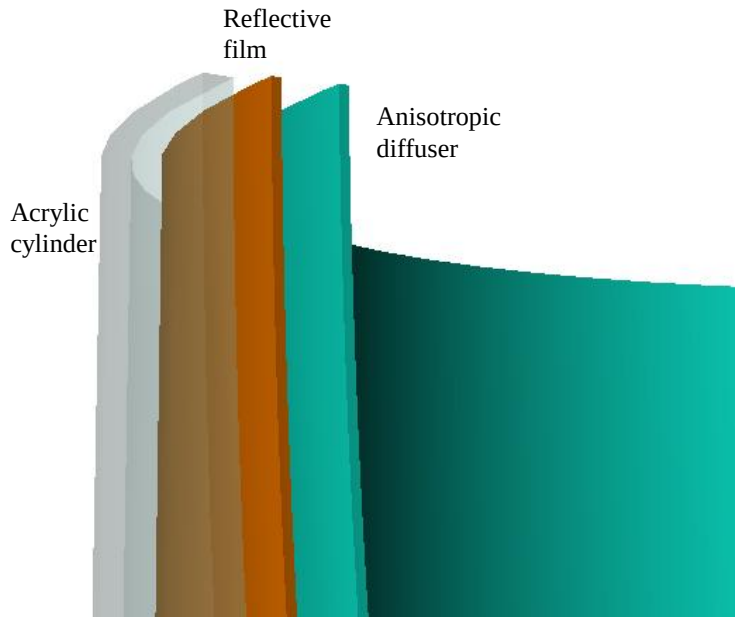

Figure 4.9 The structure of the inner surface of the cylindrical mirror.

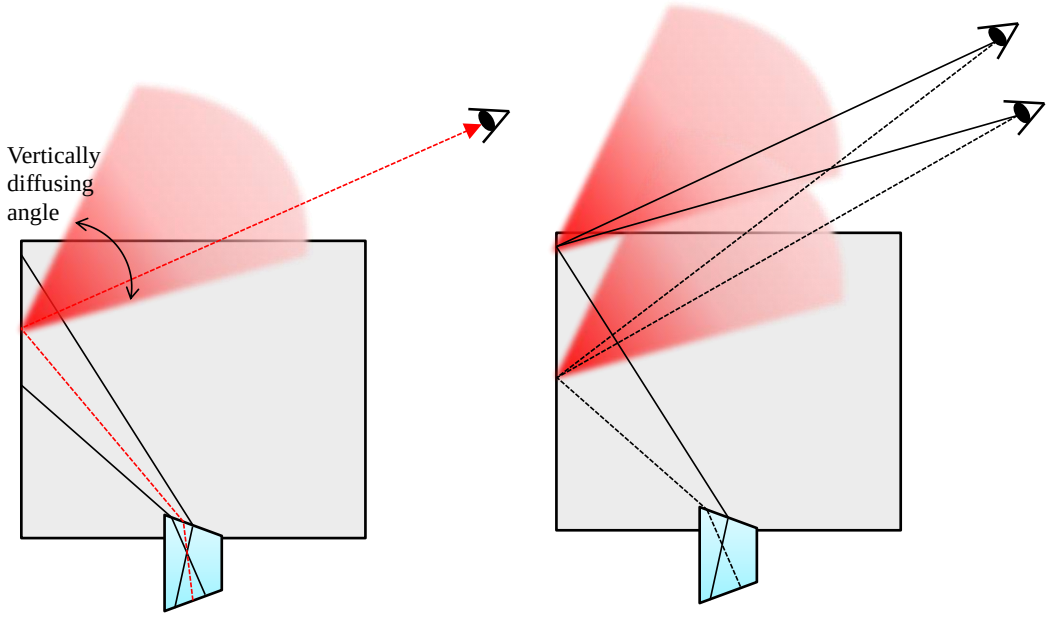

Figure 4.10 Visible areas from the vertical diffusing on the inner surface of the cylindrical mirror.

4.4. Experimental setup and results

To summarize of the experimental specification of the system, it is described in Table 4.2. As shown in the table, all base images are made by the process with 360 view images, which means that the angular interval of directional images is 1°.

Table 4.2 Experimental specification.

Cylindrical mirror	Radius	72, 127 mm
	Height	200, 370 mm
Wedge prism	Diameter	25 mm
	Deviation angle(2ea)	33°
DMD projector	Resolution	1024(H) x 768(V)
	Effective resolution	560(H) x 525(V)
	Max frame rate	13,333 Hz (@binary image)
Motor	Rotation speed	1,800 rpm
	Power	40 W
Base image	Number of views	360 ea
	Bits per a pixel	1 bit (binary)
Parameters in anamorphic transformations	d, R, θ	600, 1000, 110°

Figure 4.11 shows the overall schematic and a captured image of the whole system. This structure includes all components except only a personal computer connected with a USB interface. The overall size of the system is about 300 mm (H) x 390 mm (D) x 420 or 600 mm (V).

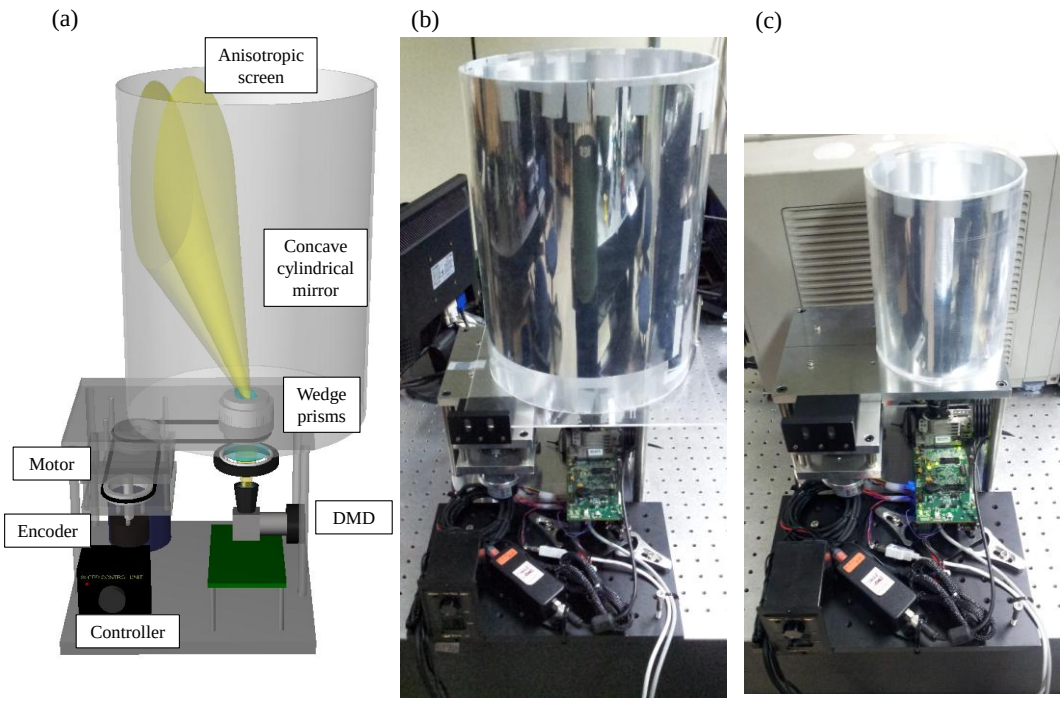

Figure 4.11 The overall schematic and images of the experimental system. (a) Main parts in the system, (b) with a big cylindrical mirror, and (c) with a small cylindrical mirror.

Figures 4.12-4.15 show the reconstruction images in the experiments. Figure 4.12 uses a simple 3D object, alphabet H with a thickness. As the position moves from the left to the right direction, it is verified that there is the motion parallax. Figure 4.13 shows the experimental results using a 3D model, chair rendered by computer graphics. Also in this case, the reconstructed images provide motion parallax of the object. Figure 4.15 is the reconstructed case with captured images of a real white ring-type object. Although there is a little distortion of the ring shape, the motion parallax can be checked by Figure 4.15(a)-(e). Three reconstructed images are provided with a big cylindrical mirror whose

diameter is 254 mm. Two reconstructed images by 3D models in Figure 4.14 are generated with a small cylindrical mirror whose diameter is 144 mm. Using a smaller cylindrical mirror, these images have less color dispersion vertically. The analysis for image quality will be mentioned in next chapter.

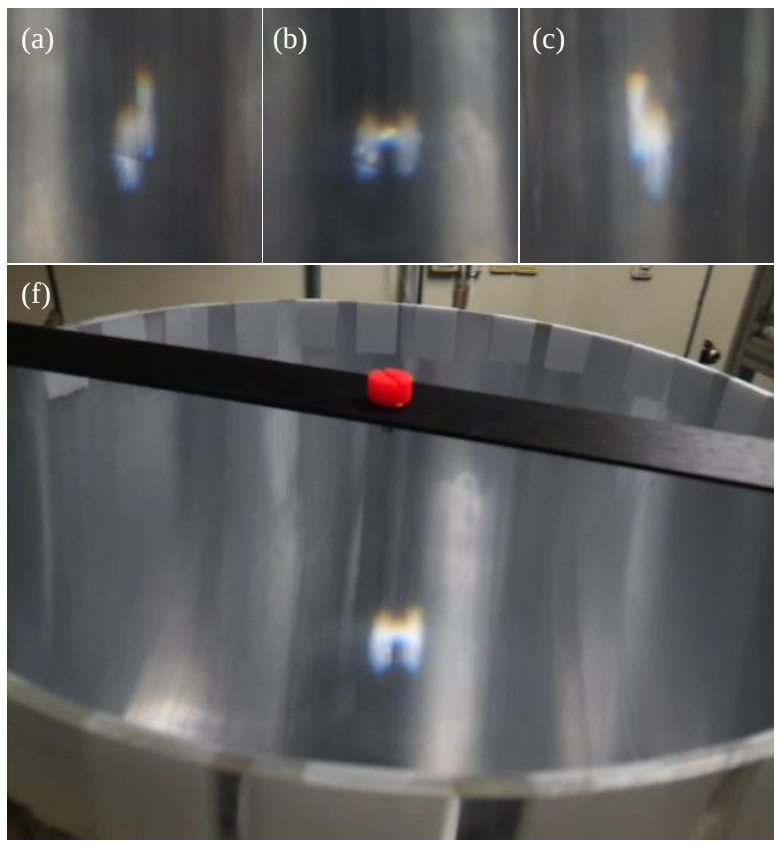

Figure 4.12 Reconstructed images of alphabet ‘H’ in a big cylindrical mirror. (a)-(c) Captured images in the left, center, and right positions, (f) captured image in a movie.

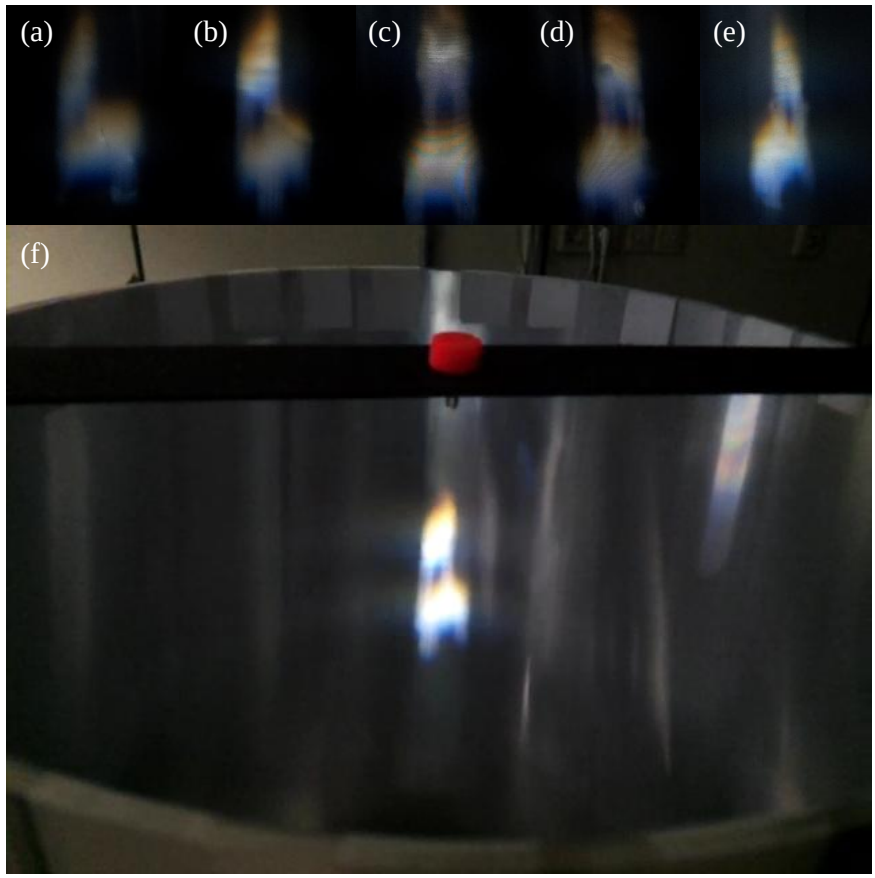

Figure 4.13 Reconstructed images of a 3D model by computer graphics, chair in a big cylindrical mirror. (a)-(e) Captured images in the five different positions around the system, (f) captured image in a movie.

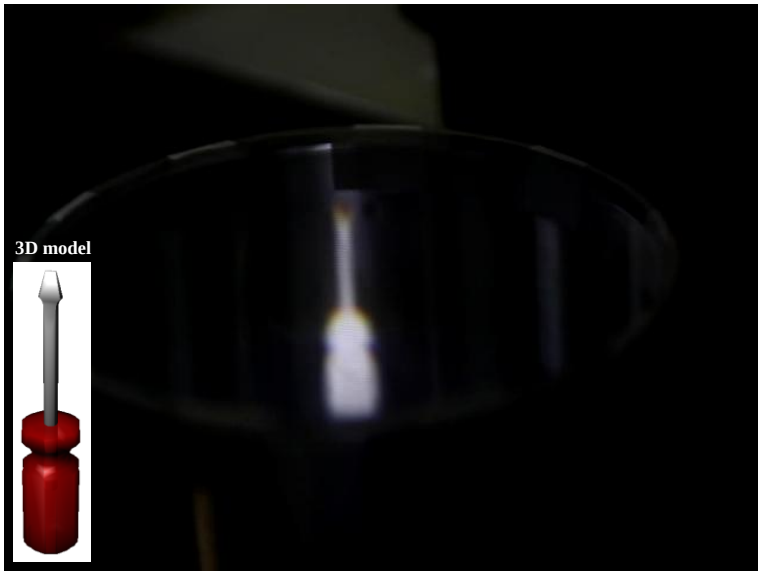

(a)

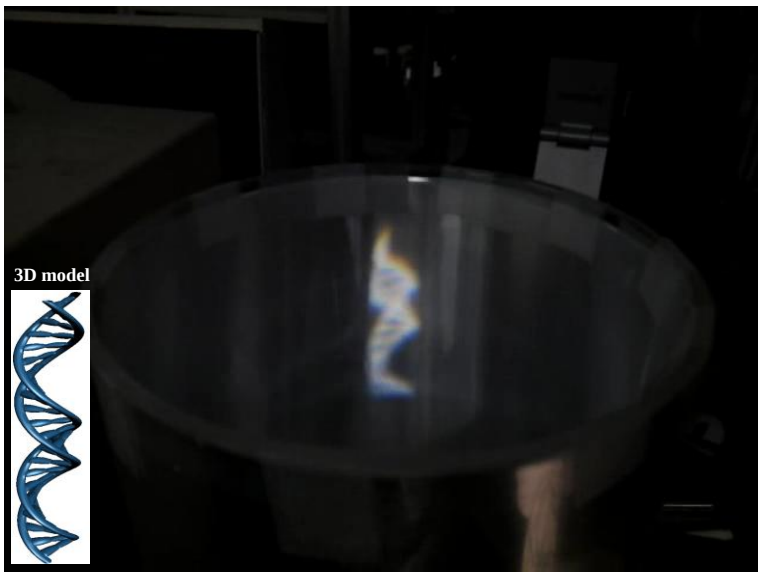

(b)

Figure 4.14 Reconstructed images of 3D models: (a) a screwdriver and (b) a DNA double helix structure in a small cylindrical mirror.

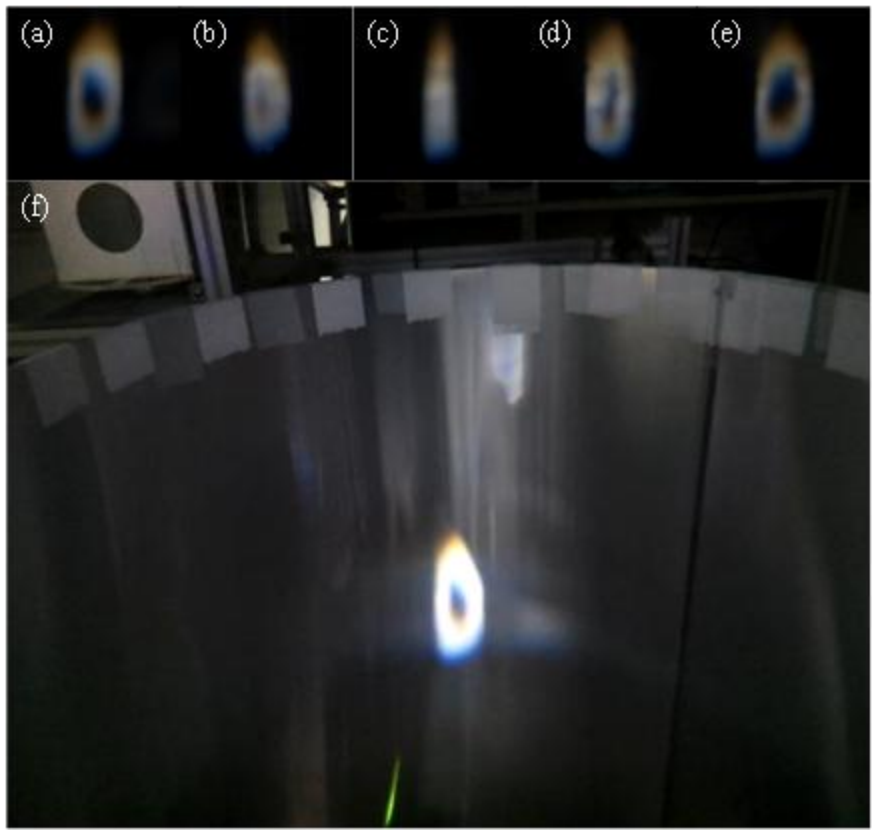

Figure 4.15 Reconstructed images of a ring-shaped real object in a big cylindrical mirror. (a)-(e) Captured images at five different positions around the system, (f) captured image in a movie.

5. Analysis of design parameters in anamorphic volumetric display

5.1. Main parameters for design of anamorphic volumetric display

Figure 5.1 shows some parameters which are concerned with the design of the system. Each parameter is decided by the deviated angle of wedge prisms δ and the radius of the cylindrical mirror R. p_w and p_h are the width and the height of the projected area on the inner surface of the cylindrical mirror. θ_{ver} and θ_{offset} including p_w and p_h are variables dependent on the deviated angle from the wedge prism and the radius of the cylindrical mirror R.

The height of the viewing area on the cylindrical mirror is decided by p_h if the vertical diffusing range of all the projected area covers the position of the observer. The p_h is linearly proportional to the radius of the cylindrical mirror as the following equation (5-1).

$$\begin{aligned} p_h &= R\left[\tan\left(\theta_{ver}+\theta_{offset}\right)-\tan\theta_{offset}\right] \\ &= R\left[\frac{1}{\tan\left(\delta\right)}-\frac{1}{\tan\left(\delta+\theta_{ver}\right)}\right] \end{aligned} \tag{5.1}$$

As for the projector, the maximal frame rate is a critical factor to define the number of views. It is because the projector should project several hundreds of view images per one rotation. Additionally, the optic axis should rotate in fast speed more than 1200 RPM.

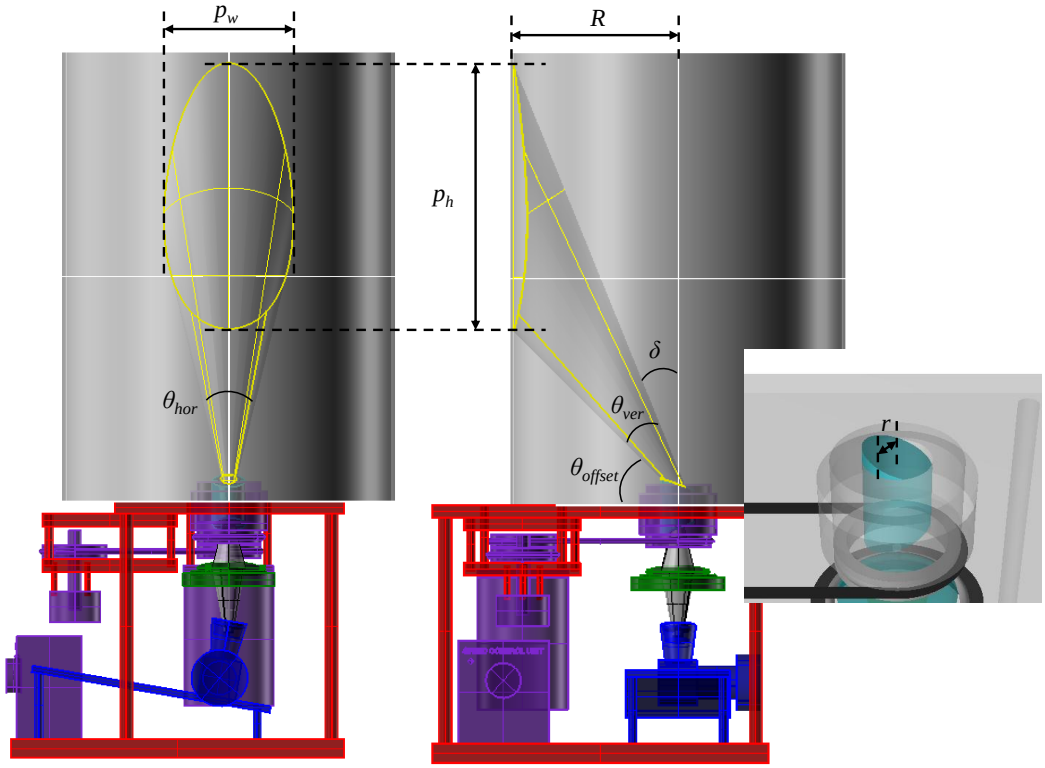

Figure 5.1 The main parameters for design of the system.

5.2. Size of image volume

In volumetric displays, image volume means the parameter representing how large 3D volume observers can watch in the systems. Especially, image volume per system resources like the resolution and the number of used images in the system can be one of criteria for evaluating the systems. In the proposed anamorphic volumetric display system, the image volume has a cylindrical shape from the cylindrical mirror which has the same structure along the every horizontal direction. Therefore, there are two parameters, the radius and the height of cylindrical image volume to estimate the size.

The image volume in the proposed system is not on a static material, but floating in the air. Although the image volume can be seen with different sizes as the position of

viewers, it can be changed significantly when the viewers are in proper regions as shown in Figure 5.3.

It is assumed that a viewer watches a 3D image in the position, (d_x, d_y) relatively from the central point of the image volume as described in Figure 5.3. Then the height of image volume, H_{volume} is defined by the height of the projected area on the cylindrical mirror as the following equation (5.2).

$$H_{volume} = \frac{d_x}{d_x + R} p_h \tag{5.2}$$

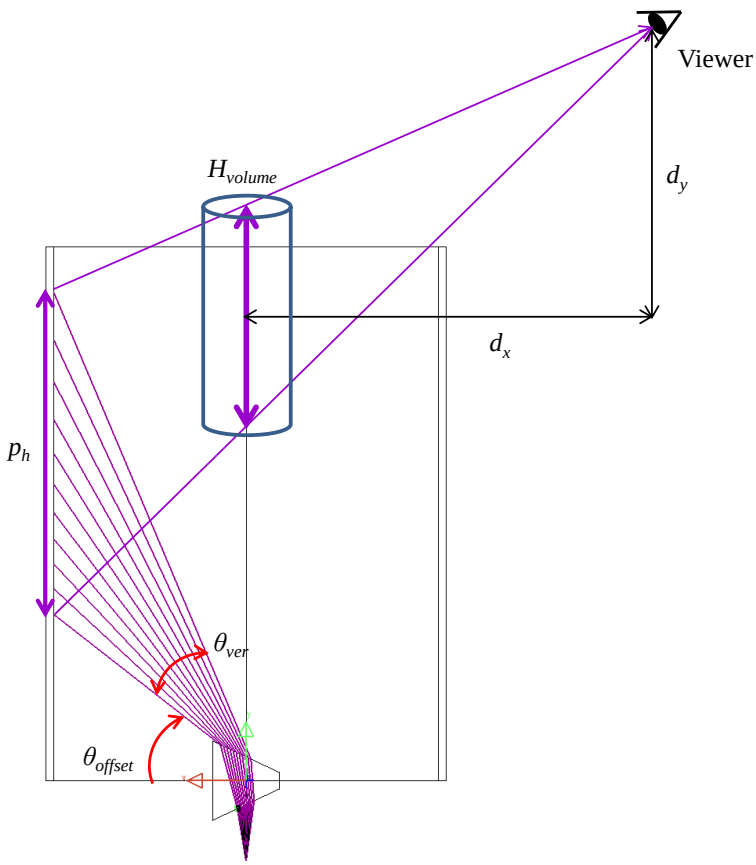

Figure 5.2 Side view of an anamorphic volumetric display system and its image volume.

Figure 5.3 shows the upper view of the projected area on the surface of the cylindrical mirror. Three parameters which can decide the radius in the horizontal cross section area of the image volume x, are the radius of the cylindrical mirror R, the radius of exit pupil r and the diverging angle θ from wedge prisms.

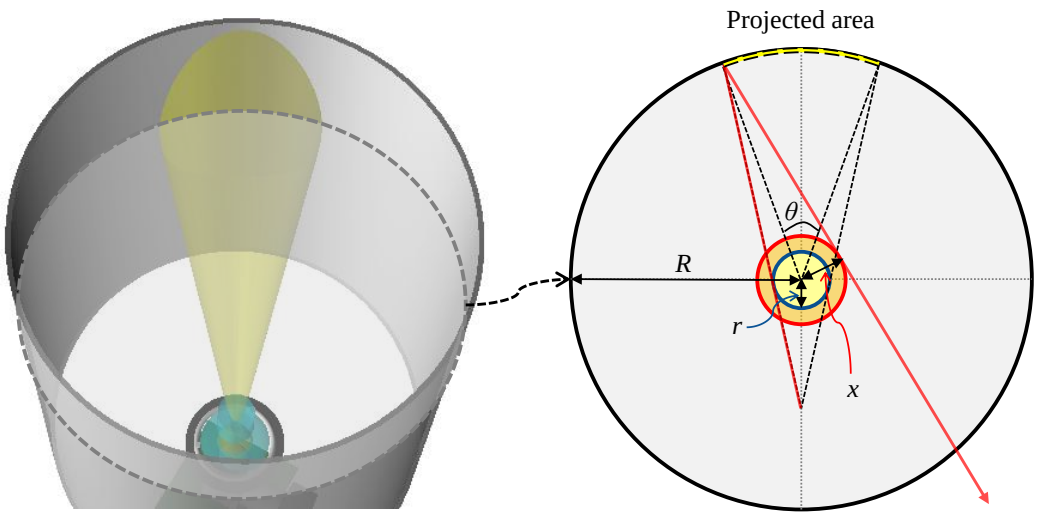

Figure 5.3 The schematic for calculation of image volume.

The radius of image volume in anamorphic volumetric display system can be induced to equation (5.2) using simple principles of reflection and geometry in Figure 5.3.

$$x = R\sin\left(\frac{\theta}{2} - \tan^{-1}\left(\tan\frac{\theta}{2} - \frac{r}{R}\sec\frac{\theta}{2}\right)\right) \tag{5.3}$$

Using the real parameters of the implemented system as shown in Figure 5.4, value of the radius of the image volume is 10.6 mm. To find the dependency of the radius of the image volume with other parameters r and θ, two graphs in Figure 5.5 andFigure 5.6 are obtained using equation (5.3). From the two graphs, two facts can be found that the radius of the image volume x is almost proportional to the radius of the exit pupil and the radius x is almost independent on the diverging angle of the projector. In other words, the radius of wedge prisms, r should be bigger to expand the horizontal range of the image volume.

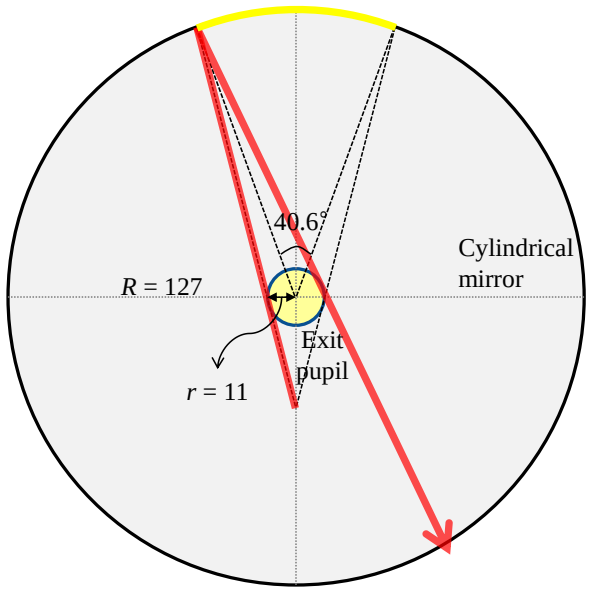

Figure 5.4 The parameter values for the image volume in the implemented system.

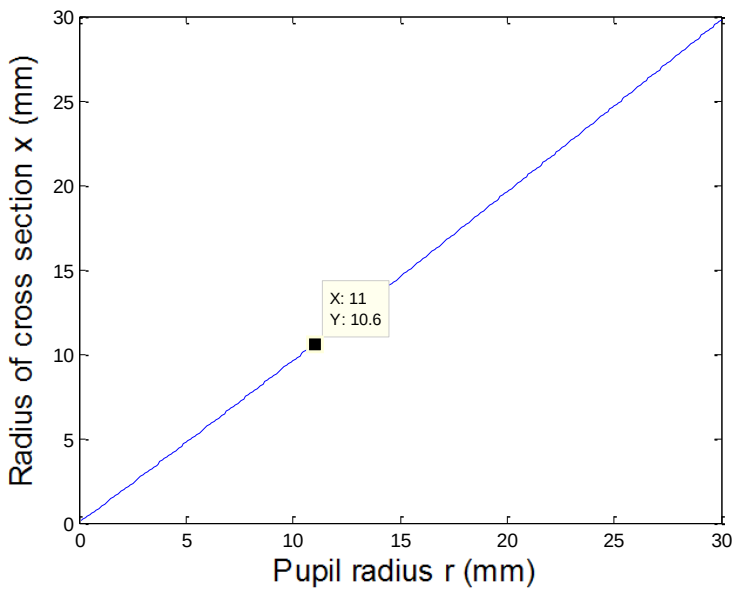

Figure 5.5 The relationship between the radius of the image volume x and the pupil radius from wedge prism r. The point on the graph means the values of the pupil radius r and the radius of horizontal cross section of the image volume, x in experiments.

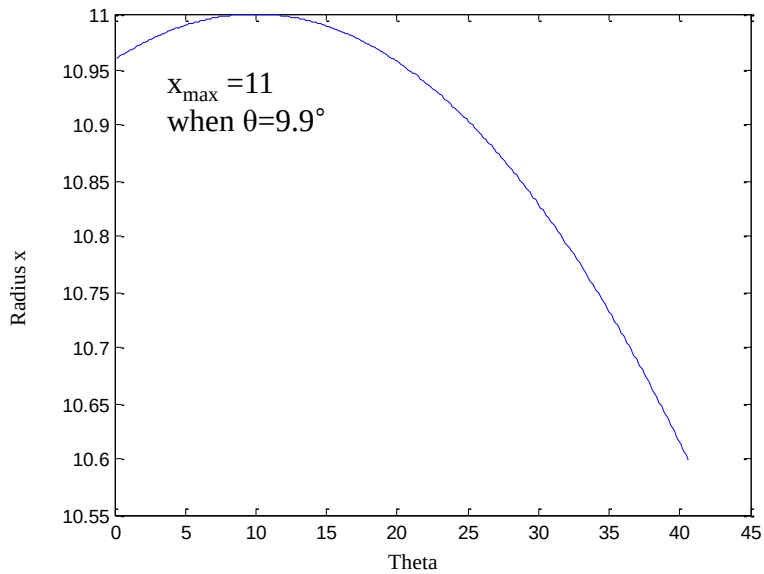

Figure 5.6 The relationship between the radius of the image volume *x* and the diverging angle *θ*.

In short, the anamorphic volumetric display systems can display 3D points in both virtual space and real space using view images to a 3D floating point in the image volume on the cylindrical mirror as shown in Figure 5.7. The whole process with the five steps from view images to base images takes about several minutes with a personal computer when the number of views is 360.

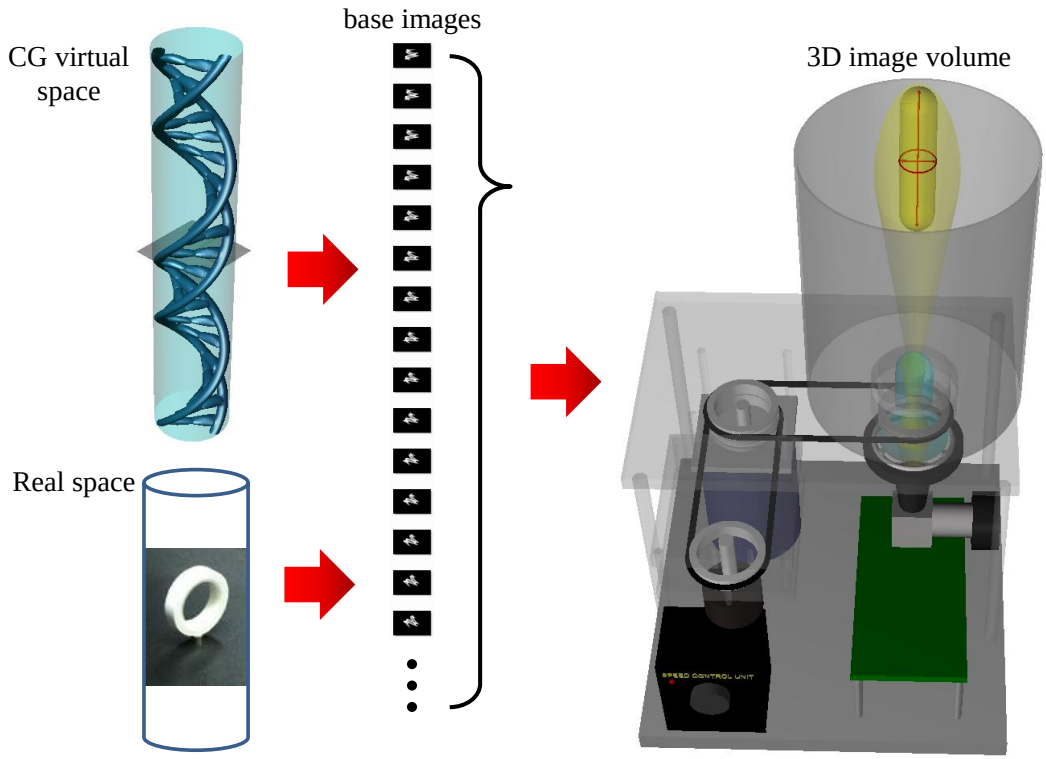

Figure 5.7 The mapping relationship from virtual space by computer graphics and real space to image volume in anamorphic volumetric display system by five steps of image calibration.

5.3. Blurring of image volume

As shown in Fig. 4.12-15, the reconstructed images in experiments are blurred significantly. Especially, cases using a big cylindrical mirror show more blurred images than cases with a small mirror. The first cause of the blur is color dispersion by using the wedge prism which deviates optic axis of incident image beams.

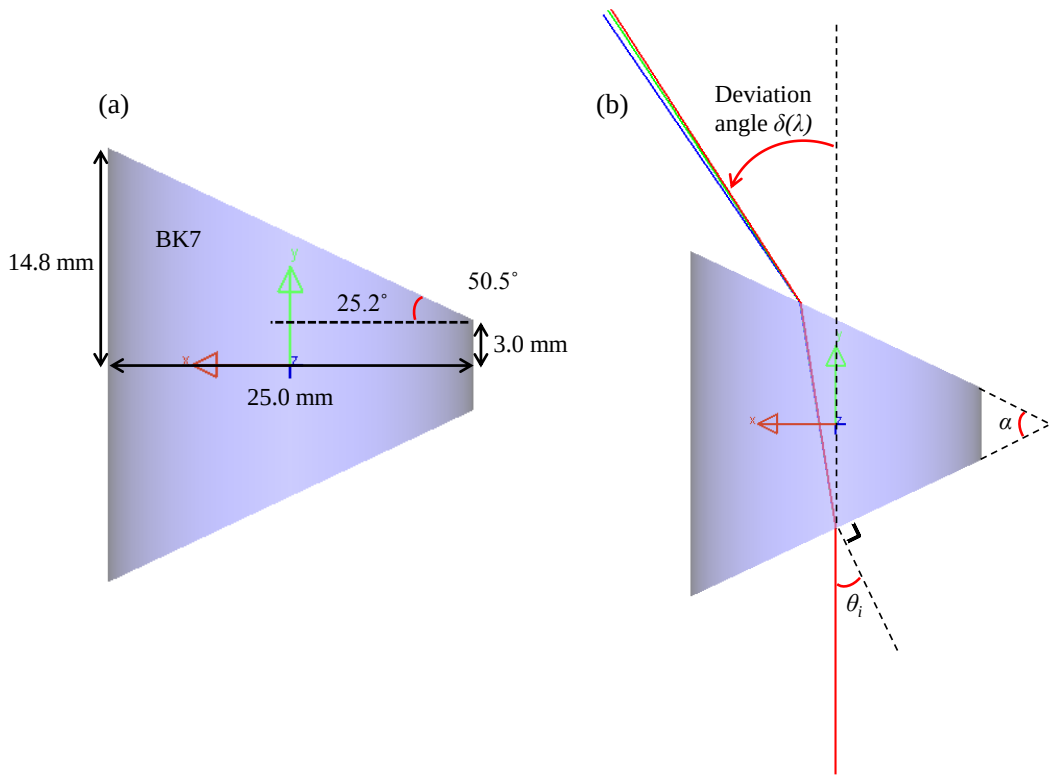

Figure 5.8 Specification of used wedge prism and diagram of color dispersion through the prism.

As described in Figure 5.8(a), two wedge prisms in the proposed system are attached with each other to form a combined wedge prism to maximize the deviation angle. However, the problem is that the deviation angle is a function for wavelengths because the refractive index of the prism is not constant over the range of visible wavelengths.

Using Figure 5.8(b), the deviation angle in each wavelength can be calculated by equation (5.4).

$$\delta(\lambda) = \theta_i + \sin^{-1}\left[(\sin\alpha)\sqrt{n(\lambda)^2 - \sin^2\theta_i} - \sin\theta_i \cos\alpha \right] - \alpha \qquad (5.4)$$

The other important thing to be considered for measuring color dispersion is the range of the light source of the projector. In the author's systems, the light source is a white LED module. Therefore, the spectrum of white LED should be considered to estimate the color dispersion. Figure 5.9(a) shows the spectrum of phosphor-based white LED which uses a blue LED and a phosphor for yellowish light. As the graph, the FWHM (Full Width at Half Maximum) is about 440 ~ 630 nm. In the range, refractive index of BK7 glass has changed from 1.526 to 1.515.

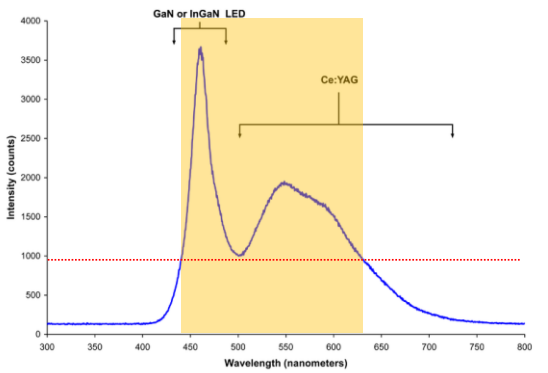

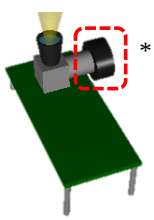

* Phosphor-based White LED

(a) White LED spectrum

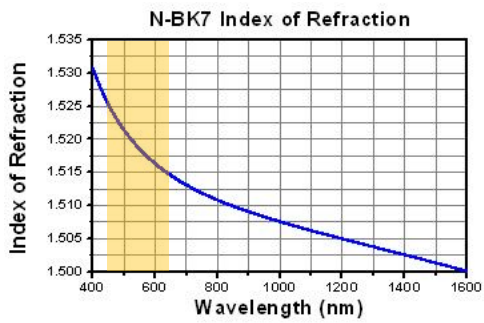

(b)

Figure 5.9 (a) Spectrum of the light source in the DMD projector [30], and (b) refractive index of BK7 along wavelength [31].

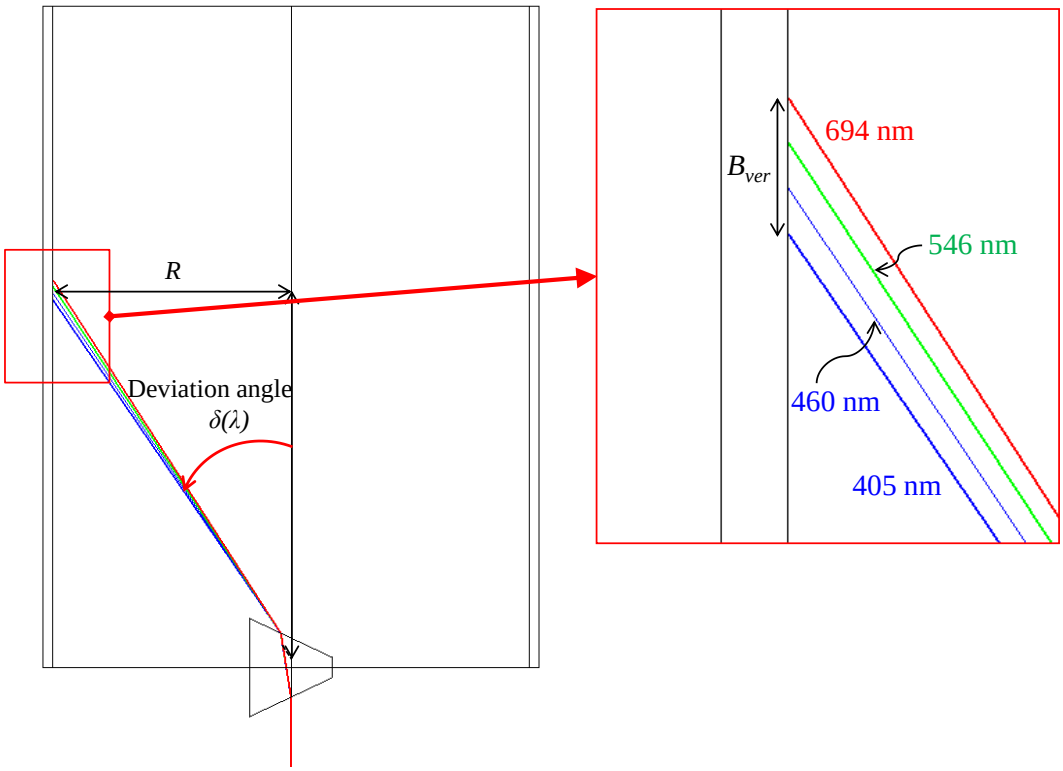

Figure 5.10 Vertical blurring distance, B_{ver} in a side view image of the proposed system.

Figure 5.10 shows a simulation result of ray tracing with different wavelengths through the BK7 wedge prism. Different refractive indexes in the range of wavelengths cause the different deviated angle, and vertical blur with the wavelengths. The vertically blurring distance, B_{ver} can be calculated by a simple formula (5.5). For example, when λ_{long}, λ_{short} are 633 nm, 442 nm, and R is 72 mm, B_{ver} is 4.5 mm.

$$B_{ver} = R\left(\frac{1}{\tan\delta(\lambda_{long})} - \frac{1}{\tan\delta(\lambda_{short})}\right) \tag{5.5}$$

The important thing is that the vertical blurring distance is proportional to the radius of the cylindrical mirror. Base on the fact, there will be about 1.8 times bigger vertical blurring distance, 8.1 mm, in the case with a big cylindrical mirror. And what should be considered is that the vertical blurring distances are seen to viewers with the ratio in

(5.2). Figure 5.11 shows two reconstructed images in both cylindrical mirrors. Vertical blurring in a bigger cylinder mirror is longer than in a smaller cylinder mirror.

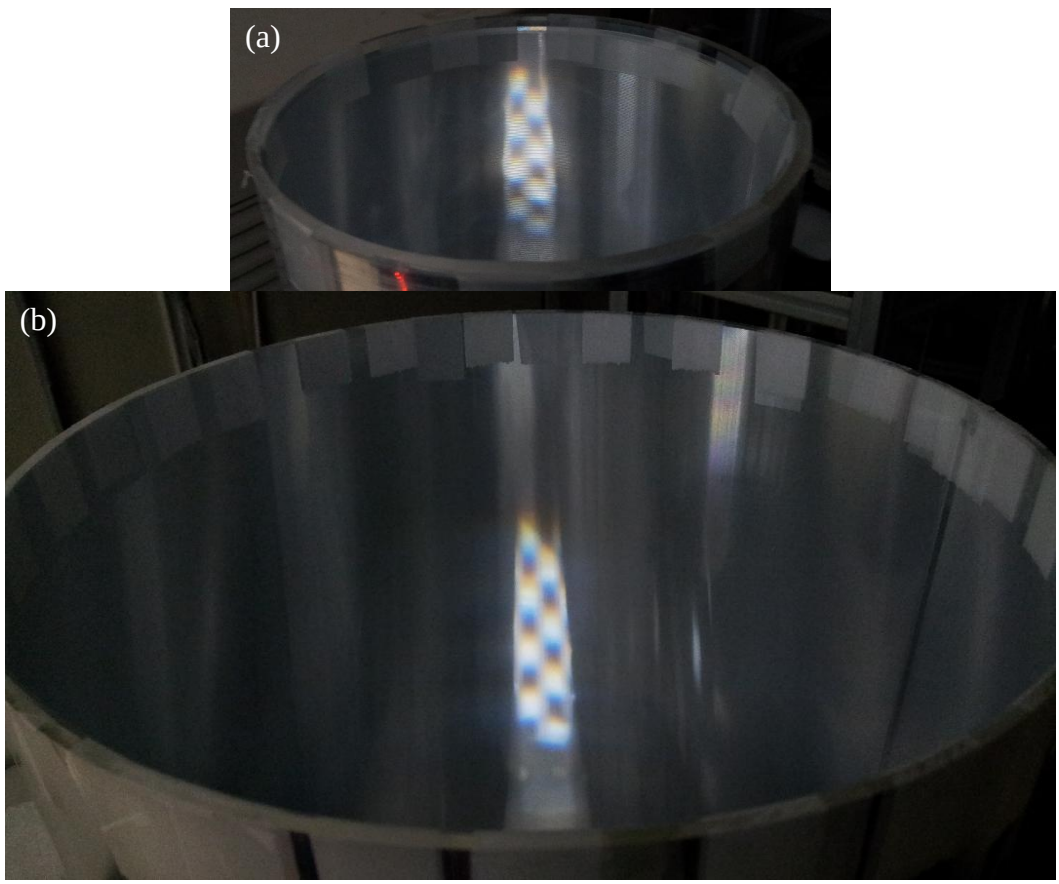

Figure 5.11 Comparison of color dispersion between the same pattern images in cylindrical mirrors with different radii, (a) 72mm, (b) 127mm.

In addition, Figure 5.12 shows an additional comparison with reconstructed images of the same real object in both cylindrical mirrors. Figure 5.12(a)-(c) are reconstructed images using a big cylindrical mirror with the radius of 127 mm. Those have remarkably bigger blurring in vertical direction than in a smaller cylindrical mirror with the radius of 72 mm.

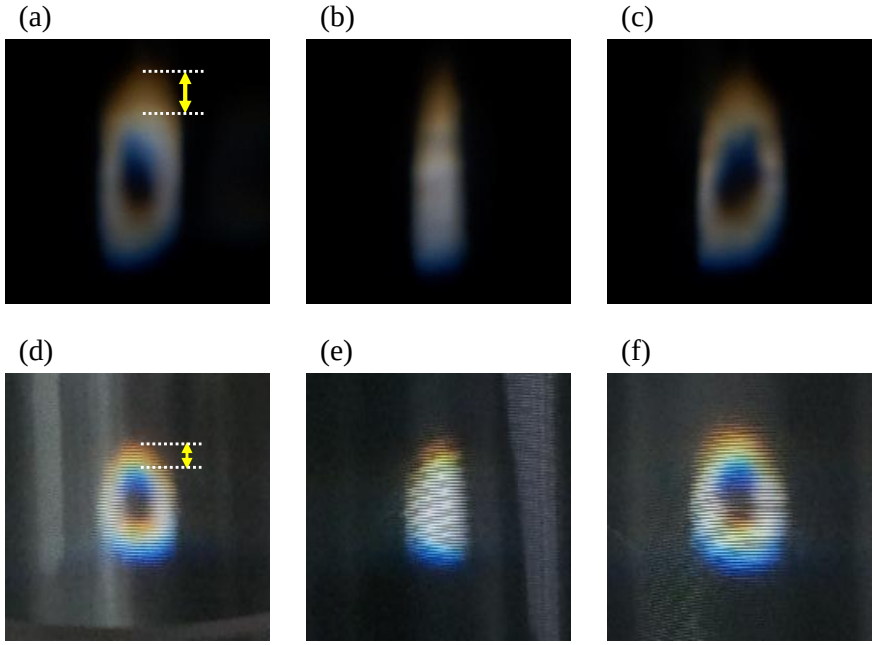

Figure 5.12 Comparison of color dispersion between the reconstructed real images in cylindrical mirrors with different radii, (a)–(c) 127 mm, (d)-(f) 72 mm.

On the other hand, horizontal blurring cannot be explained with color dispersion. One of candidates for horizontal blurring is scanning in an exposed time of each image. To look into the scanning in the short time, a top view image is described in Figure 5.13. The figure shows that a point P_1 matches another point P_3 after reflection on the cylindrical mirror by a reflection formula (5.6).

$$\overrightarrow{P_2P_3} = 2((N \cdot \overrightarrow{P_1P_2})N) - \overrightarrow{P_1P_2} \tag{5.6}$$

The formula (5.6) gives the coordinates of point P_3 as a following matrix equation (5.7). This can also be understood as axial symmetry with N vector on point P_2. As the equation, the reflected rays from point P_1 should go through point P_3 which is on the same radius with the point P_1.

$$\begin{pmatrix} x_3 \\ y_3 \end{pmatrix} = \begin{pmatrix} \cos 2\theta & \sin 2\theta \\ \sin 2\theta & -\cos 2\theta \end{pmatrix} \begin{pmatrix} x_1 \\ y_1 \end{pmatrix} \tag{5.7}$$

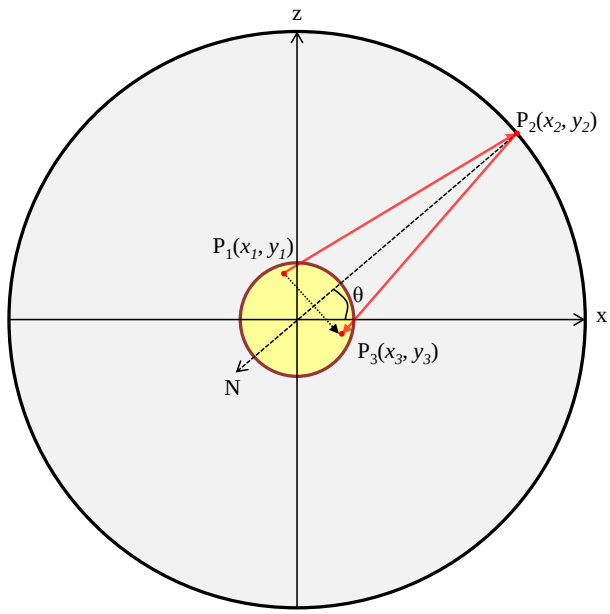

Figure 5.13 Corresponding point by reflection on the cylindrical mirror.

Therefore, the point P_3 moves the same distance as the distance which point P_1 moves in one exposed time. The exposed time of the projector is inversely proportional to the number of views because the projector should project in faster speed. The moving distance of points within the exit pupil of the wedge prism can be calculated with equation (5.8) using only the number of views N_{view}, and the radial distance of the points from an original point r_p.

$$l = \frac{\pi}{180} r_p d\theta = \frac{\pi}{180} r_p \times \frac{360}{N_{view}} = \frac{2\pi r_p}{N_{view}} \tag{5.8}$$

Figure 5.14 shows that moving distances of the points P_1 and P_3 are identical. However, since viewers cannot recognize the point P_3 on a ray going through a space, the distance l can be seen bigger like that the point P_3 is located in the nearer boundary to the viewer. For example using real values of N_{view} (360 ea), r_p (11 mm), the distance l is 0.19 mm which is relatively small with vertical blur or observed horizontal blur as shown in Figure 5.11 or Figure 5.12. In the case for the maximal value of l as described in Figure 5.15, the value of l can be 0.26 mm, which is still so short distance.

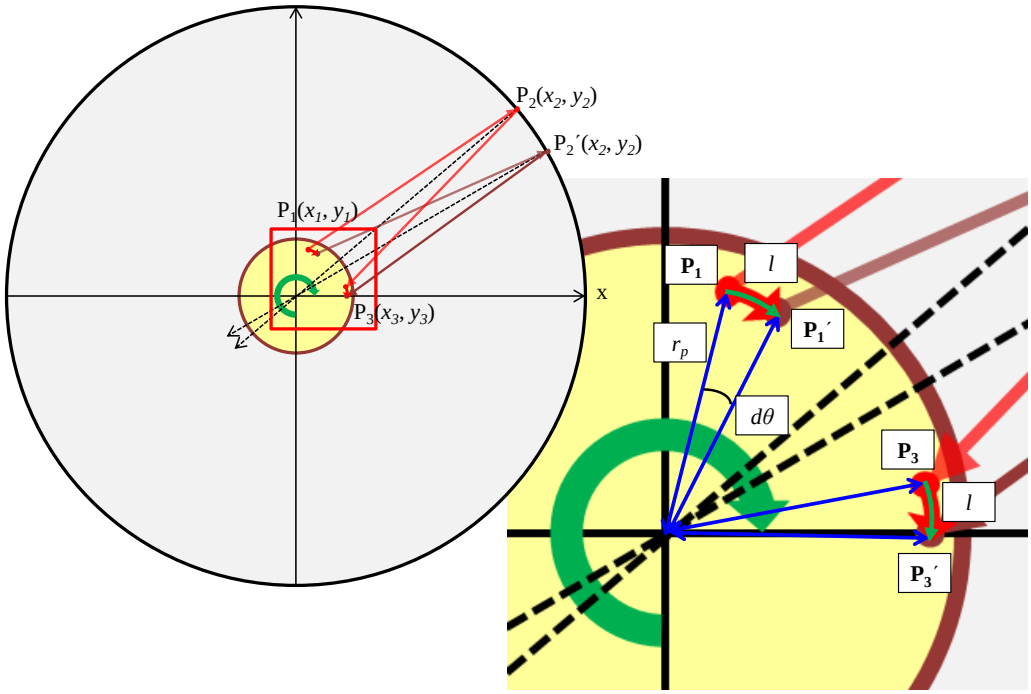

Figure 5.14 Scanning distance of each point before and after reflections.

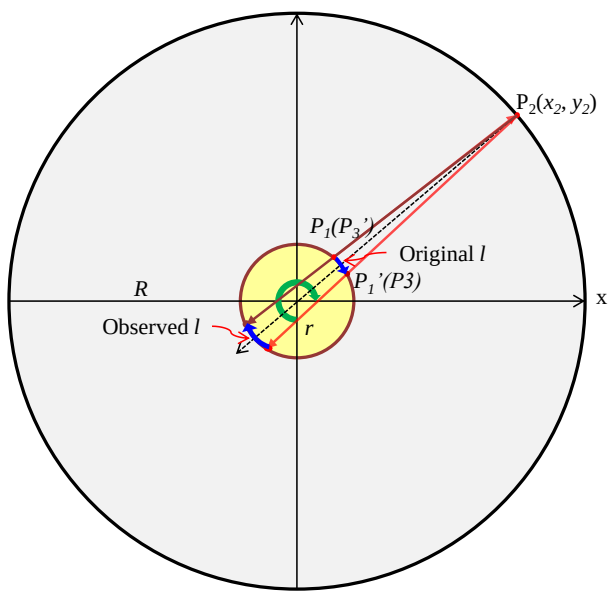

Figure 5.15 The case for the maximal value of the distance *l*.

The other cause for horizontal blurring is concerned with the depth of focus of the projector. Depth of focus with a projector means a range in depth direction where acceptable sharpness exists. The depth of focus region is perpendicular to the optic axis. Therefore, in the proposed system with the wedge prism, the depth of focus region is located obliquely with the inner plane of the cylindrical mirror as shown in Figure 5.16. For this reason, the sharpness on the projected area can be dulled according to the projected position.

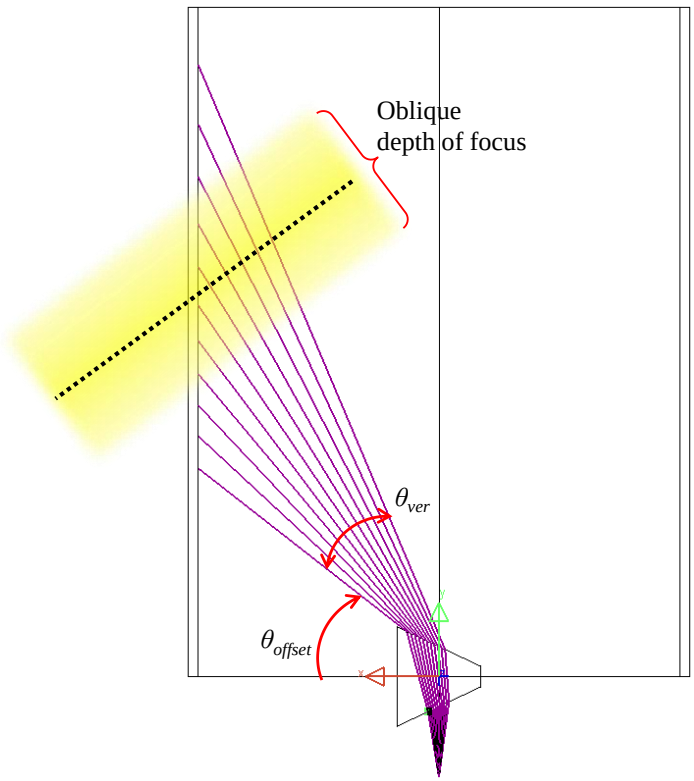

Figure 5.16 Oblique depth of focus against the inner plane of the cylindrical mirror.

5.4. Applications

In contrast with conventional stereoscopic or multi-view 3D display systems, anamorphic volumetric display systems have some distinctive characteristics. One of them is that multiple viewers can watch 3D images simultaneously in every horizontal direction. And the proposed system has small moving parts with small vibration. However, it cannot provide images with high quality. Therefore, this system seems not proper to be used as display devices playing 3D movies or 3D games.

Some of the candidates for good applications are 3D modeling, 3D video communication, medical education, science education, architectural design, and so on. All of these applications have the common-several persons can talk with 3D images on business, education or conversations.

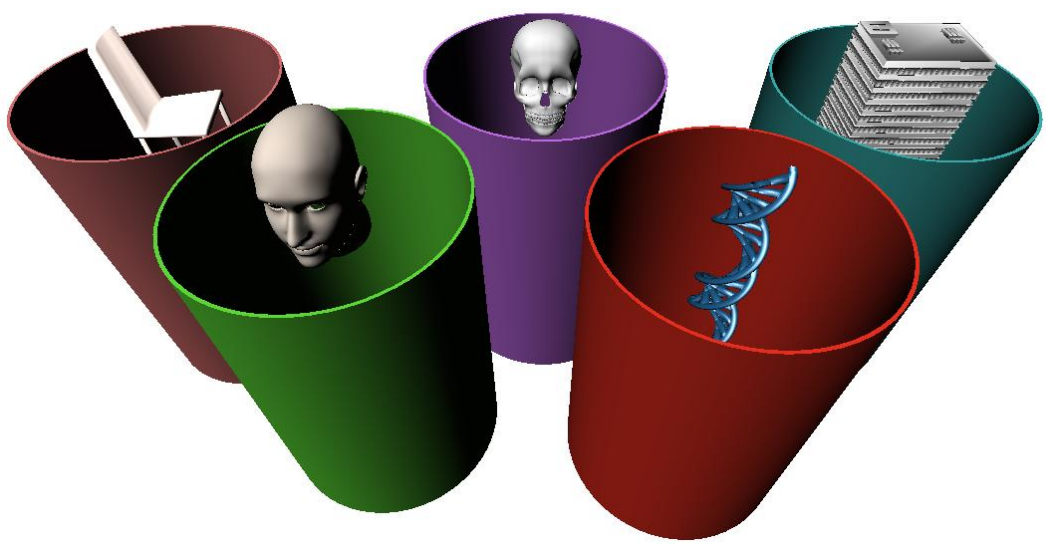

Figure 5.17 Five examples of applications, 3D modeling, 3D video communication, medical education, science education, and architectural design.

6. Summary and conclusion

The aim of this dissertation was to show novel possibilities in volumetric display systems using the principle of anamorphosis which is the way to distort images to show in strange illusory ways with curved surfaces. Among several kinds of curved surfaces like cylinders, cones, spheres, etc, a cylindrical mirror has a structure which can converge diverging rays from projectors by reflection. To make 3D floating images in the air, there should be intersecting rays in the air. Converging rays by the cylindrical mirror can be used to make intersecting rays for 3D images. There are two systems using cylindrical mirrors in this dissertation. One is anamorphic floating display system introduced in Chapter 2. The other one is anamorphic volumetric display system which is discussed from Chapters 3 to 5.

In Chapter 2, anamorphic floating display system is introduced as the fundamental panoramic display system using a cylindrical mirror without any diffuser. It means that the light emitting from each pixel on a monitor goes forward in every direction above the monitor. Therefore observers should be in the specific position to watch intended floating images. However, it is shown that the small resources with tracking technology can be used to make floating images which seem like 3D images in every horizontal direction. Tracking technology and image mapping method are integrated to provide panoramic floating images in real time. However, tracking technology has a limitation that it cannot track more than one or two persons simultaneously with limited resources.

Anamorphic volumetric display system is motivated from the goal which is the volumetric display system whose 3D images can be seen to multiple viewers without tracking or glasses. Three chapters from Chapters 3 to 5 cover image calibration processes, hardware implementation using a DMD projector, and analysis of the system.

In Chapter 3, anamorphic volumetric display system is proposed with a simple structure of the system and the method for calibration images in five steps. Generation method of images for the anamorphic volumetric display system, which are called base

images, is verified with experimental results in each step. Image processing in five steps costs about 3 minutes to make 360 base images avoiding unnecessary calculations.

In Chapter 4, the hardware components in the system are discussed in more detail from a high-speed projector to a cylindrical mirror with an anisotropic diffuser. There are not many options to choose the commercialized high-speed projector. Since a DMD projector can project more than 10,000 frames per second, the projector can be used to project 3D floating images with the frame rate, 30Hz, though projected images have only binary data. Spinning wedge prisms are the alternatives for replacing rotating screens or mirrors with minimizing moving parts. And after we made two cylindrical mirrors with different radii, we could recognize the differences between them concerning with image quality, the size of image volume, and so on.

In Chapter 5, we analyzed the system for important parameters which define the size of image volume or determine blurring. There are many parameters in every hardware and software components. However, it is important which parameters are critical to define the performance of the system. One of the most important performances is the size of image volume. Among some parameters including diverging angle from wedge prisms, the size of exit pupil in wedge prisms, and the radius of a cylindrical mirror, it is found that the two parameters except the size of exit pupil do not affect the size of image volume directly. The maximum size of exit pupil from the wedge prism is the diameter of the wedge prism. It shows that a wedge prism or other alternatives with bigger diameters should be used for large image volume. Lastly, the author discussed which are the causes of blurring of 3D images both horizontally and vertically. In the case of vertical blurring, color dispersion from the wedge prism is the main factor to induce blurred images. It can be checked with calculations considering the refractive indexes of the wedge prism and the bandwidth of light sources for the projector. In the case of horizontal blurring, some candidates like image scanning and depth of focus are discussed as the causes.

The basic performance of the proposed system is limited by the limitation of each component like a DMD projector, a light source, wedge prisms and so on. The first limitation from the projector is the fact that only mono binary images can be projected in such high speed. Gray-level expressions can be imitated with binary images using half-

toning method which is the technique that simulates continuous brightness with binary images. We applied half-toning method to several objects. However, there was no significant enhancement in the expression of gray-level images. It is probably resulted from large amount of blurring effects. The second limit is the spectrum of the light source. If the bandwidth is narrow, the vertical blurring effect from color dispersion can be reduced remarkably. And the third limit is the radius of a wedge prism which is almost the same as the radius of image volume. However, it is difficult to use wedge prisms with large diameters because of the vibration of the prisms. What can be considered as alternatives for wedge prisms are an off-axis Fresnel lens and electro-wetting prisms. Anamorphic volumetric display systems with some enhancements mentioned above are expected to be able to be used in several applications in near future.

Bibliography

[1] A. Boev, D. Hollosi, A. Gotchev, and K. Egiazarian, "Classification and simulation of stereoscopic artifacts in mobile 3DTV content," in *Electronic Imaging*, 2009.

[2] Y. Kajiki and H. Yoshikawa, "Hologram-Like video images by 45-view stereoscopic display," in *SPIE 3012*, 1997.

[3] Y. Takaki and N. Nago, "Multi-projection of lenticular displays to construct a 256-view super multi-view display," *Optics Express,* vol. 18, no. 9, pp. 8824-8835, 2010.

[4] B. G. Blundell and A. J. Schwarz, "The classification of volumetric display systems: characteristics and predictability of the image space," *IEEE TRANSACTIONS ON VISUALIZATION AND COMPUTER GRAPHICS,* vol. 8, no. 1, pp. 66-75, 2002.

[5] O. S. Cossairt, J. Napoli, S. L. Hill, R. K. Dorval, and G. E. Favalora, "Occlusion-capable multiview volumetric three-dimensional display," *Applied Optics,* vol. 46, no. 8, pp. 1244-1250, 2007.

[6] A. Sullivan, "A solid-state multi-planar volumetric display," in the Society for Information Display, 2003.

[7] H. H. Refai, "3D images using cspace display for air traffic control applications," *Journal of Display Technology,* vol. 7, no. 4, pp. 186-192, 2011.

[8] E. Downing, L. Hesselink, J. Ralston, and R. Macfarlane, "A three color, solid-state, three dimensional display," *Science,* vol. 273, pp. 1185-1189, 1996.

[9] A. Rapaport, J. Milliez, M. Bass, A. Cassanho, and H. Jenssen, "Review of the properties of up-conversion phosphors for new emissive displays," *Journal of Display Technology,* vol. 2, no. 1, pp. 68-78, 2006.

[10] S. DiVerdi, I. Rakkolainen, T. Hollerer, and A. Olwal, "A novel walk-through 3D

display," in *SPIE Electronic Imaging, Stereoscopic Displays and Applications XVII*, San Jose, CA, USA, 2006.

[11] G. Favalora, R. K. Dorval, D. M. Hall, M. Giovinco, and J. Napoli, "Volumetric three-dimensional display system with rasterization hardware," in *SPIE Stereoscopic Displays and Virtual Reality VIII*, San Jose, CA, USA, 2001.

[12] K. Langhans, D. Bahr, D. Bezecny, D. Homann, K. Oltmann, K. Oltmann, C. Guill, E. Rieper, and G. Ardey, "FELIX 3D Display: An Interactive Tool for Volumetric Imaging," in *Photonics West*, San Jose, CA, USA, 2002.

[13] A. Jones, I. McDowall, H. Yamada, M. Bolas, and P. Debevec, "Rendering for an Interactive 360 degrees light field display," in *ACM SIGGRAPH*, 2009.

[14] Y. Takaki and S. Uchida, "Table screen 360-degree three-dimensional display using a small array of high-speed projectors," *Optics Express,* vol. 20, no. 8, pp. 8848-8861, 2012.

[15] D. Miyazaki, K. Ohno, and T. Mukai, "Real-time updatable volumetric display system based on inclined-image scanning," in *Sixth International Conference on Intelligent Information Hiding and Multimedia Signal Processing*, 2010.

[16] C. Yan, X. Liu, D. Liu, J. Xie, X. X. Xia, and H. Li, "Omnidirectional multiview three-dimensional display based on direction-selective light-emitting diode array," *Optical Engineering,* vol. 50, no. 3, pp. 034003-1~6, 2011.

[17] J. L. Hunt, B. G. Nickel, and C. Gigault, "Anamorphic images," *American Journal of Physics,* vol. 68, no. 3, pp. 232-237, 2000.

[18] M. G. Tomilin, "Anamorphoses - Optical oddities of the renaissance or sources of the science of image processing?," *Journal of Optical Technology,* vol. 68, no. 9, pp. 723-726, 2001.

[19] F. Solina and B. Batagelj, "Dynamic anamorphosis," in *4th International Conference on Enactive Interfaces*, Grenoble, France, 2007.

[20] J.-E. Lee, S. Miyashita, K. Azuma, J.-H. Lee, and G.-T. Park, "Anamorphosis projection by ubiquitous display in intelligent space," in *The 5th International*

Conference on Universal Access in Human-Computer Interaction, 2009.

[21] "Art of anamorphosis, software," [Online]. Available: http://www.anamorphosis.com/software.html.

[22] "Morph-O-Scopes," [Online]. Available: http://oozandoz.com.

[23] S. Pastoor, "Human factors of 3D displays in advanced image communications," *Displays,* vol. 14, no. 3, pp. 150-157, 1993.

[24] S. Adhya and J. Noe, "A complete ray-trace analysis of the 'Mirage' toy," in *ETOP*, 2007.

[25] C. Cruz-Naira, D. J. Sandin, and A. T. DeFanti, "Surrounded-screen projection-based virtual reality: the design and implementation of the CAVE," in *ACM SIGGRAPH*, 1993.

[26] M. Agrawala, B. A. C., B. Frohlich, P. Hanrahan, I. McDowall, and M. Bolas, "The two-user responsive workbench: support for collaboration through individual views of a," in *ACM SIGGRAPH*, 1997.

[27] R. Haussler, S. Reichelt, N. Leister, E. Zschau, R. Missbach, and A. Schwerdtner, "Large real-time holographic displays: from prototypes to a consumer product," in *SPIE 7237*, 2009.

[28] G. E. Favalora and O. S. Cossairt, "Theta-parallax-only (TPO) displays". United States Patent 7364300, 29 Apr. 2008.

[29] "Wikipedia," [Online]. Available: http://en.wikipedia.org/wiki/wedge_prism.

[30] "Wikipedia," [Online]. Available: http://en.wikipedia.org/wiki/Light-emitting_diode.

[31] "THORLABS," [Online]. Available: http://www.thorlabs.de.

한글 초록

본 논문은 왜상 기법을 사용하는 새로운 3 차원 디스플레이 시스템들을 제안하였다. 3 차원 영상 정보의 디스플레이를 위한 방법으로는 안경식과 무안경식 3 차원 디스플레이, 체적형 디스플레이, 홀로그래피 등과 같은 다양한 기술의 수많은 연구가 진행중이다. 이러한 3 차원 디스플레이 기술은 3 차원 영상을 재생하기 위해 2 차원 디스플레이보다 훨씬 많은 양의 정보를 사용한다. 그러나 디스플레이에 사용되는 소자들의 한계로 인해서 많은 연구들이 기존 소자들을 순차적 혹은 공간적으로 다중화하는 기법을 사용한다.

본 논문에서 제안한 시스템 중 하나는 원통거울과 추적기술을 사용한 왜상 부유형 디스플레이 시스템이다. 원통거울은 축방향으로 볼록렌즈와 같은 역할을 한다. 이를 이용해 2 차원 디스플레이 패널의 영상을 공간상에 띄우고, 관찰자는 원통거울 위에 떠 있는 영상을 볼 수 있게 된다. 본 시스템에서 관찰자에게 운동 시차를 제공하기 위해서는 추적기술을 사용하여 관찰자의 위치에 따라 다른 영상을 디스플레이한다. 이에 따라 관찰자는 위치에 따라 다른 방향의 영상을 보게 되고, 3 차원 물체가 원통거울 위에 떠 있는 것처럼 인식할 수 있다.

그리고, 본 논문은 고속의 DMD 프로젝터와 원통거울, 왜상 프리즘, 이방성 확산판을 사용한 왜상 체적형 디스플레이 시스템을 제안하였다. 이 시스템에서 DMD 프로젝터는 수 백개의 방향으로 그 수만큼의 방향별 영상을 고속으로 투사하는 역할을 한다. 그리고 원통거울은 프로젝터에서 투사된 영상들이 반사되어 원통거울의 축방향으로 띄우도록 한다. 이 때, 프로젝터로부터 투사되는 영상이 각기 다른 방향으로 투사되도록 하기 위해서는 모터로 회전 구동이 되는 왜상 프리즘이 사용되었다. 왜상 프리즘은 프리즘을 통과하는 영상의 투사방향이 기울어지도록 한다. 이러한 왜상 프리즘을 회전시키면, 수직으로 투사된 영상이 왜상 프리즘을 통과한 후 기울어진 투사방향으로의 영상이 원통거울의 안쪽면을 따라 투사되도록 할 수 있다. 이 때, 원통거울에서 반사되는 영상은 원통거울의 곡면에 의해 왜곡된다. 이 영상의 왜곡은 왜상의 원리와 유사하며, 왜곡을 없애기 위해 역으로 왜곡시킨 영상을 다섯 단계의 보정과정을 이용하여 생성하고, 이를

프로젝터를 통해 투사시킨다. 프로젝터의 출사동의 크기와 확산각은 관찰자 위치의 세로 범위를 충족시키기에는 크지 않기 때문에, 관찰자가 원통거울을 직접 바라보게 되면 제대로 된 영상이 아닌 1 차원 형태의 영상들만을 보게 된다. 이 문제를 해결하기 위해서 이방성 확산판을 원통거울의 안쪽면에 부착하여 반사되는 영상이 세로방향으로 확산이 되도록 하였다. 각 구성 품목의 자세한 설명과 사양은 본 논문에 소개되었으며, 실험 결과들도 함께 제공되었다.

주요어 : 3 차원 디스플레이, 체적형 디스플레이, 원통거울, 쐐기형 프리즘, DMD 프로젝터

학번 : 2008-30874